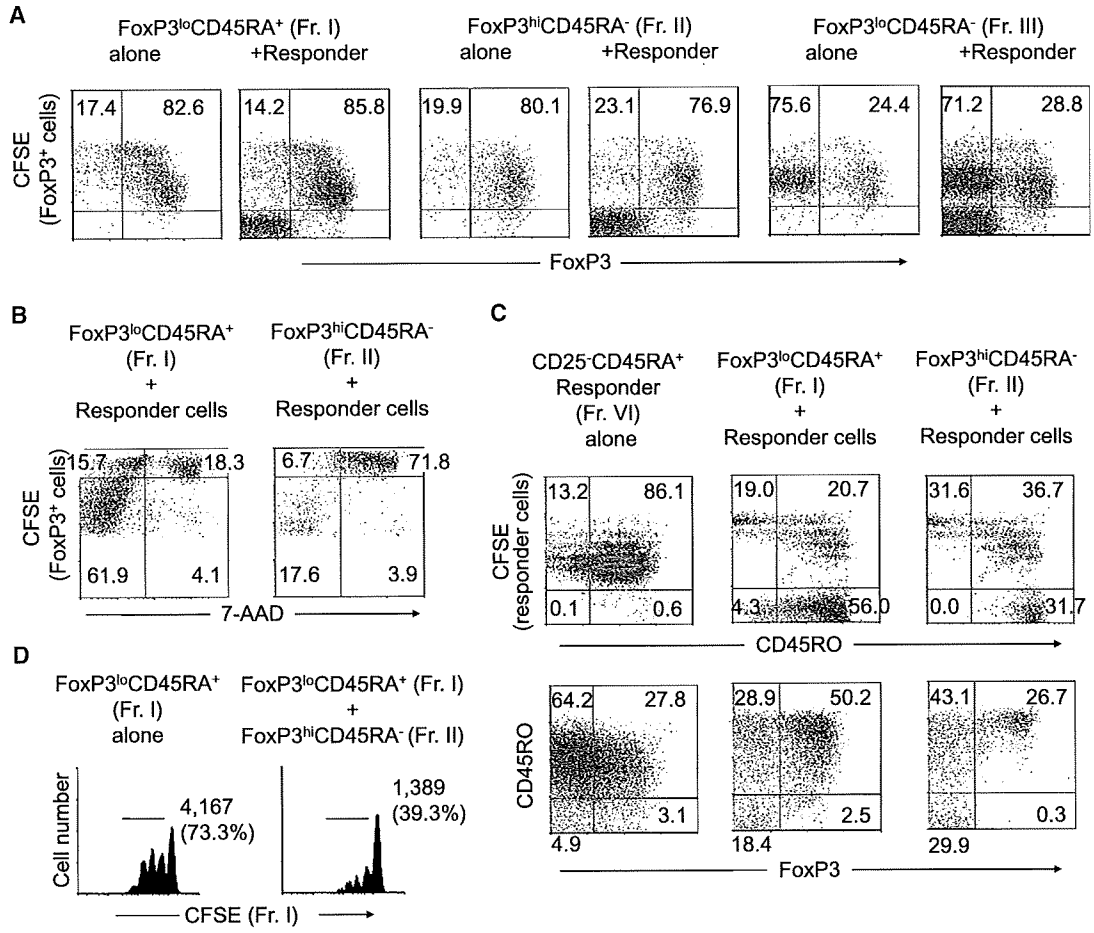

Figure 3. In Vitro Properties of FoxP3+ Subpopulations

(A) CFSE dilution by rTreg or aTreg cells and intracellular expression of FoxP3 were analyzed after 4 days TCR stimulation in the absence or presence of nonlabeled responder cells. Percentages of $FoxP3^-$ and of $FoxP3^+$ cells among CFSE-labeled cells are indicated.

(B) Viability assessed by 7-AAD staining of CFSE-labeled $CD45RA^+FoxP3^{lo}$ (left) or $CD45RA^-FoxP3^{hi}$ Treg cells (right) cocultured with nonlabeled responder cells for 4 days. Only CFSE-labeled cells are shown. Numbers indicate percentage in each quadrant. Data shown are representative of five independent experiments.

(C) CFSE dilution, surface CD45RO, and intracellular FoxP3 expression by CFSE-labeled responder cells cultured alone or cocultured with unlabeled Treg cell subsets for 4 days. Numbers indicate percentage in each quadrant.

(D) CFSE dilution of labeled rTreg cells cultured alone or with aTreg cells at a 1 to 1 ratio. Numbers and percentage of proliferating cells are indicated. Data shown in (B) and (D) are representative of five independent experiments.

(Fr. II) and rTreg cells (Fr. I) gave rise to CFSE-diluting $FoxP3^+$ cells when cultured alone (Figure 3A). In addition, rTreg cells showed more active proliferation than did aTreg cells in the presence of responder cells. In contrast with rTreg or aTreg cells, most (~70%) of $CD45RA^-FoxP3^{lo}CD4^+$ T cells (Fr. III) did not express FoxP3 during their proliferation, indicating that FoxP3 expression in the majority of Fr. III cells may not be stable in concordance with the methylation status of their *FOXP3* gene (Figure 3A).

Based on the finding that very few aTreg cells (Fr. II) were detectable after 4 days of culture (Figure S7), we assessed the viability of Treg cells by measuring incorporation of 7-AAD by CFSE-labeled rTreg or aTreg cells cultured with responder cells (Figure 3B). The majority (~75%) of aTreg cells were positive for 7-AAD. By contrast, although a fraction (~20%) of rTreg cells were nonproliferative and 7-AAD^+, the majority of proliferating rTreg cells (~60%) were 7-AAD^- (Figure 3B). In addition to proliferation, rTreg cells showed increased expression of FoxP3 (Figure 3A), CD45RO (Figure 3C), and intracellular CTLA-4 (Figure S8). High expression of CD45RO was secondary to activation because rTreg cells, which were $CD45RA^+$, did not express CD45RO when freshly isolated from peripheral blood (Figure S9). Further, when CFSE-labeled rTreg cells (Fr. I) were cultured with nonlabeled aTreg cells (Fr. II), the latter substantially suppressed the proliferation of the former (Figure 3D).

Taken together, rTreg cells are not anergic and are able to proliferate upon TCR stimulation. They acquire a $Ki\text{-}67^+FoxP3^{hi}$ aTreg cell phenotype and exert suppression during and after their proliferation and conversion to aTreg cells, which die after proliferation and exertion of suppression. Activated Treg cells also suppress the proliferation of resting Treg cells in a negative feedback fashion. Thus, in addition to different cell surface phenotypes, rTreg and aTreg cells possess different cell fates despite their comparable in vitro suppressive activity when assessed separately.

In Vivo Conversion of rTreg Cells to aTreg Cells and Differentiation of a Small Fraction of FoxP3− Cells to FoxP3+ Cells

Next, to investigate whether the in vitro conversion of rTreg cells to aTreg cells could also occur in vivo, we transferred human PBMCs containing CFSE-labeled $CD4^+$ T cells into NOG (Nod-scid-common γ-chain-deficient) mice and analyzed their splenocytes 5 days after transfer (Hiramatsu et al., 2003). $FoxP3^{hi}CD4^+$ T cells recovered in the recipients were largely $CD25^{hi}$ and $CD45RO^+$ (data not shown) and mostly confined to $Ki\text{-}67^+$CFSE-diluting cells, which had divided more than 6 times after transfer (Figure 4A). In addition, most $CD4^+$ T cells expressing low amounts of FoxP3 had not proliferated. These findings correspond to the in vitro findings that $FoxP3^{hi}$ aTreg cells found in PBMCs were highly proliferative and that $FoxP3^{lo}CD4^+$ T cells were $Ki\text{-}67^-$ in PBMCs (Figure 1E), suggesting that, upon activation, rTreg cells upregulate FoxP3 expression and then proliferate. We also examined the behavior of Treg cells or whole $FoxP3^+$ cells when injected without other effector $CD4^+$ T cells. Neither population proliferated, indicating that the maintenance and proliferation of FoxP3-expressing cells requires the presence of other $CD4^+$ T cells in vivo (Figure S10).

Similar analysis of PBMCs containing CFSE-labeled rTreg cells, prepared as shown in Figure 1A and Figure S1, showed that they proliferated in vivo and upregulated the expression of FoxP3 and CD45RO along several cell divisions (Figure 4B and data not shown). Because most $FoxP3^{hi}$ cells were detected in CFSE-negative cells after transfer of CFSE-labeled $CD4^+$ T cells or rTreg cells (Figures 4A and 4B), we attempted to determine whether rTreg cells were the major source of CFSE-negative $FoxP3^{hi}$ cells. Injection of PBMCs containing CFSE-labeled $CD4^+$ T cells devoid of rTreg cells revealed a much lower number of $FoxP3^{hi}$ cells when compared with injection of whole $CD4^+$ T cells, indicating that most $FoxP3^{hi}$ aTreg cells derive from rTreg cells (Figure 4C).

Further, to investigate whether the conversion of $FoxP3^-$ to $FoxP3^+$ in $CD4^+$ T cells could occur in vivo, we transferred PBMCs containing CFSE-labeled $FoxP3^-$ $CD127^{hi}CD4^+$ T cells together with nonlabeled $FoxP3^+$ cells (as $CD25^{hi}CD127^{lo}$ cells) in NOG mice and examined whether $FoxP3^-CD4^+$ T cells could upregulate FoxP3 in vivo (Figure 4D). Although most CFSE-labeled cells remained $FoxP3^-$, a small number of cells upregulated FoxP3 from low to high amounts. Injection of only CFSE-labeled $CD4^+FoxP3^-$ cells confirmed that a small fraction (<1%) of $CD4^+FoxP3^-$ cells indeed divided at least 6 times to give rise to $FoxP3^{hi}$ cells (Figure 4E). Taken together, these results indicate that rTreg cells convert to aTreg cells and that only a small fraction of aTreg cells derives from $FoxP3^-CD4^+$ non-Treg cells in vivo.

In Vivo Conversion of rTreg Cells to aTreg Cells in a Normal Human Individual

To obtain further evidence for the in vivo rTreg to aTreg cell conversion in normal humans, we attempted to trace clonotypes of each Treg cell fraction in a single individual at separate time points. Cells in rTreg cells (Fr. I), aTreg cells (Fr. II), and also $FoxP3^-$ non-Treg $CD4^+$ T cells (Fr. IV, V, VI) that expressed the same TCRBV5 family were sorted from a single healthy individual at 18 month intervals. Single-cell RT-PCR and DNA sequencing of the amplicons was performed to compare TCRBV5 CDR3 regions in each sorted subset. Given the small size of the sample, the analysis was able to monitor dominant clones only. First, we observed that rTreg (Fr. I) and aTreg (Fr. II) cell subsets shared few dominant clonotypes at a given time point. Second, we found that a clonotype initially detected in the rTreg cell subset was found dominant 18 months later in the aTreg but not in the rTreg cell subset. The TCR repertoire being potentially so heterogeneous and the sample size being so limited (45 to 137 cells analyzed in each subset), it is highly improbable that T cell clones with identical TCR sequences could be found in the same subsets only by chance. Indeed, when random samples of conventional $CD4^+$ T cells were similarly compared, shared clonotypes were never found in this individual (Figure 5; Table S2). The analysis also revealed that none of the clonotypes found in $FoxP3^-$ cells was found in aTreg cells 18 months later, indicating that if conversion of $FoxP3^-CD4^+$ T cells ever occurs in vivo, it may not be a frequent phenomenon compared with the conversion of rTreg cells to aTreg cells (Figure 5).

Based on these observations in Figures 4 and 5, we conclude that most $FoxP3^{hi}$ aTreg cells are derived from recently activated and vigorously proliferating rTreg cells, and that only a minority of aTreg cells can develop from $FoxP3^-CD4^+$ non-Treg cells in vivo. The result also indicates that the TCR repertoire of Treg cells, in particular that of aTreg cells, adaptively changes in normal individuals.

Variations in Human rTreg and aTreg Cell Populations under Normal and Disease Conditions

We then attempted to determine whether the dissection of $FoxP3^+$ T cells in adult humans into Fr. I–III based on CD45RA and FoxP3 expression was pertinent to the analysis of the dynamics of Treg cell generation and differentiation in ontogeny, aging, and disease states.

Although rTreg cells were highly prevalent in cord blood, we could easily detect $Ki\text{-}67^+FoxP3^{hi}CD45RA^-CD4^+$ T cells that corresponded to aTreg cells in adults. We failed to confirm the previously reported finding that all $CD25^+CD4^+$ T cells were $FoxP3^+$ in cord blood (Fritzsching et al., 2006). However, $CD4^+$ T cells expressing the highest amounts of CD25 contained only $FoxP3^+$ cells and CD127 expression efficiently separated $FoxP3^+CD25^+$ from $FoxP3^-CD25^+CD4^+$ T cells (Figure 6A). IFN-γ production was barely detectable in whole $CD4^+$ T cells whereas IL-2 production was observed in $FoxP3^{lo}CD45RA^-CD4^+$ T cells as in adults (data not shown).

Analysis of the expression of CD31 (PECAM-1), which is known to be expressed in recent thymic emigrants but lost during their post-thymic peripheral expansion (Kimmig et al., 2002), revealed that almost all $CD31^+FoxP3^+CD4^+$ T cells in adult PBL were confined in the $CD45RA^+FoxP3^{lo}$ population (Fr. I). This finding suggests that the majority of rTreg cells may be recently derived from the thymus (Figure 6B).

The proportion of rTreg cells (Fr. I) among $CD4^+$ T cells was decreased in aged donors (1.1% ± 0.59%, n = 12 versus 2.40% ± 0.89% in healthy donors, n = 29; $p < 0.0001$) whereas that of aTreg cells (Fr. II) was increased (2.48% ± 1.07% versus 1.63% ± 0.53%; $p = 0.01$; Figures 6C and 6D).

We next applied our new definition of $FoxP3^+$ T cell subsets to the analysis of two pathological conditions that reportedly show

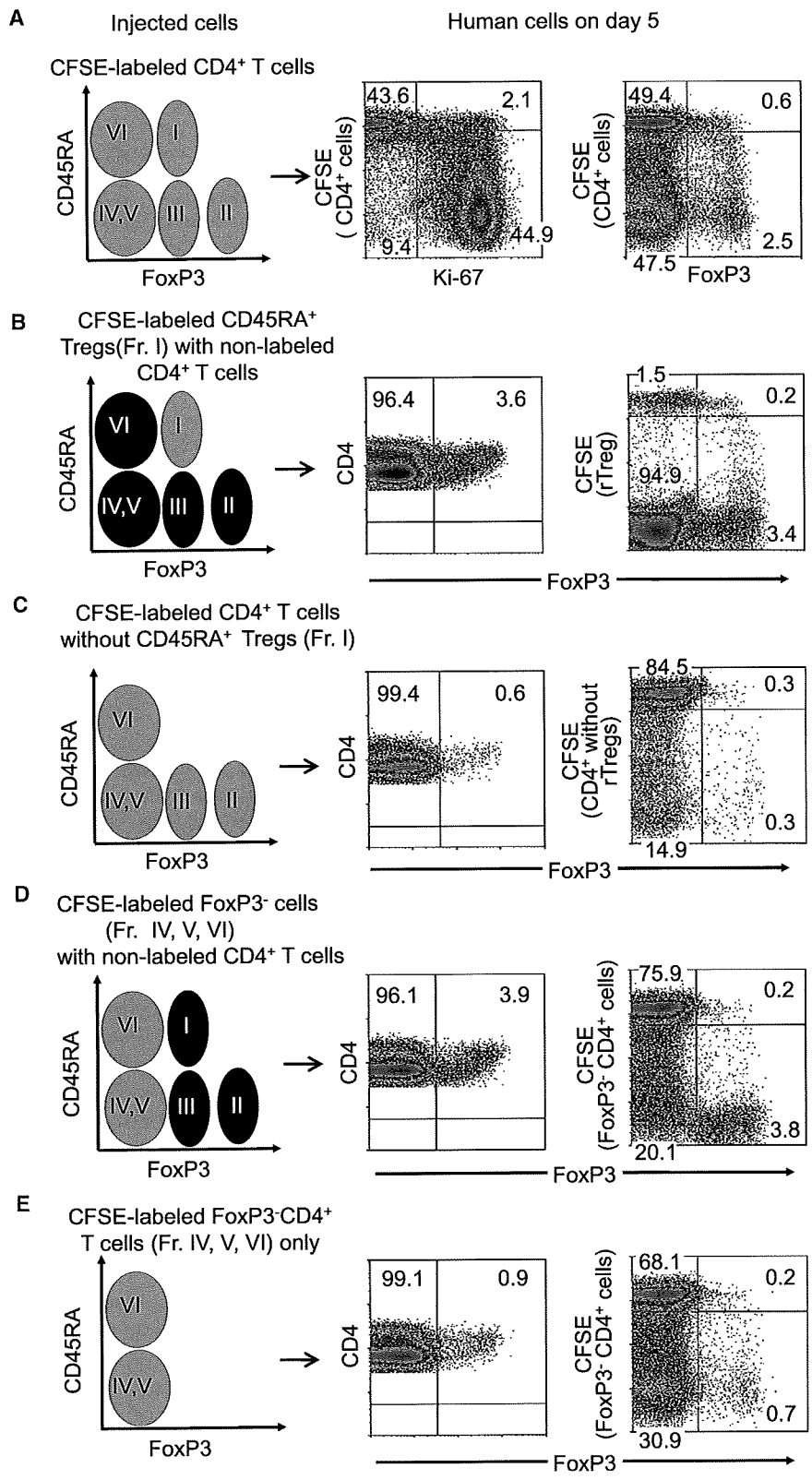

Figure 4. In Vivo Conversion of Treg Cell Phenotype in NOG Mice

PBMCs containing human CD4+ T cells were i.v. injected in NOG mice and collected in the spleen 5 days later. In schematic representations (left) of flow cytometric profiles of injected cells before transfer, CFSE-labeled CD4+ T subsets are depicted in green and injected with nonlabeled cells in black. Flow cytometry of human CD4+ T cells in the spleen after transfer of PBMCs containing CFSE-labeled human whole CD4+ T cells (A) or indicated CFSE-labeled CD4+ T cell subpopulations (B–E) into NOG mice. Numbers indicate percentage in each quadrant (right). Representative data of four mice transferred with PBMCs containing CFSE-labeled CD4+ T cells isolated from three different donors (A), and mice (two for each condition) transferred with PBMCs with indicated CFSE-labeled T cell populations obtained from two different donors (B–E).

different patterns of Treg cell involvement (Miyara et al., 2005, 2006). In sarcoidosis, a granulomatous disease of unknown origin, patients with active disease showed a considerable increase in the proportion of aTreg cells among CD4+ T cells (4.67% ± 3.35%, n = 41; $p < 0.0001$) combined with a high prevalence of Ki-67+FoxP3^{hi}CD4+ T cells and a decrease in the proportions of rTreg cells (1.48% ± 0.89%; $p < 0.0001$). In active systemic lupus erythematosus (SLE), a prototype of systemic autoimmune disease, there was a decrease in the proportion of aTreg cells (1.24 ± 0.72; n = 15; $p = 0.006$) and an increase in the proportions of rTreg cells (4.2 ± 1.86; $p = 0.0008$). Notably, CD45RA$^-$FoxP3^{lo} non-Treg cell fraction (Fr. III) increased to form a distinct population in active SLE (10.37% ± 9.3% versus 3.04 ± 1.1 in healthy donors; $p < 0.0001$; Figures 6C and 6D).

Thus, distinction of Treg cell subsets simply based on the combination of CD45RA and FoxP3 expression is highly informative in assessing the dynamics of Treg cell differentiation under physiological and disease conditions.

DISCUSSION

We have shown in this report that FoxP3+ cells in human PBL are heterogeneous in function and include not only suppressive T cells but also nonsuppressive ones that abundantly secrete proinflammatory cytokines such as IL-17. Further, Treg cells functionally and phenotypically differentiate within the FoxP3+ population. This functional heterogeneity and differentiation dynamics can be clearly shown by separating FoxP3+ cells into three subsets based on the expression of FoxP3 and CD45RA (or CD45RO), which

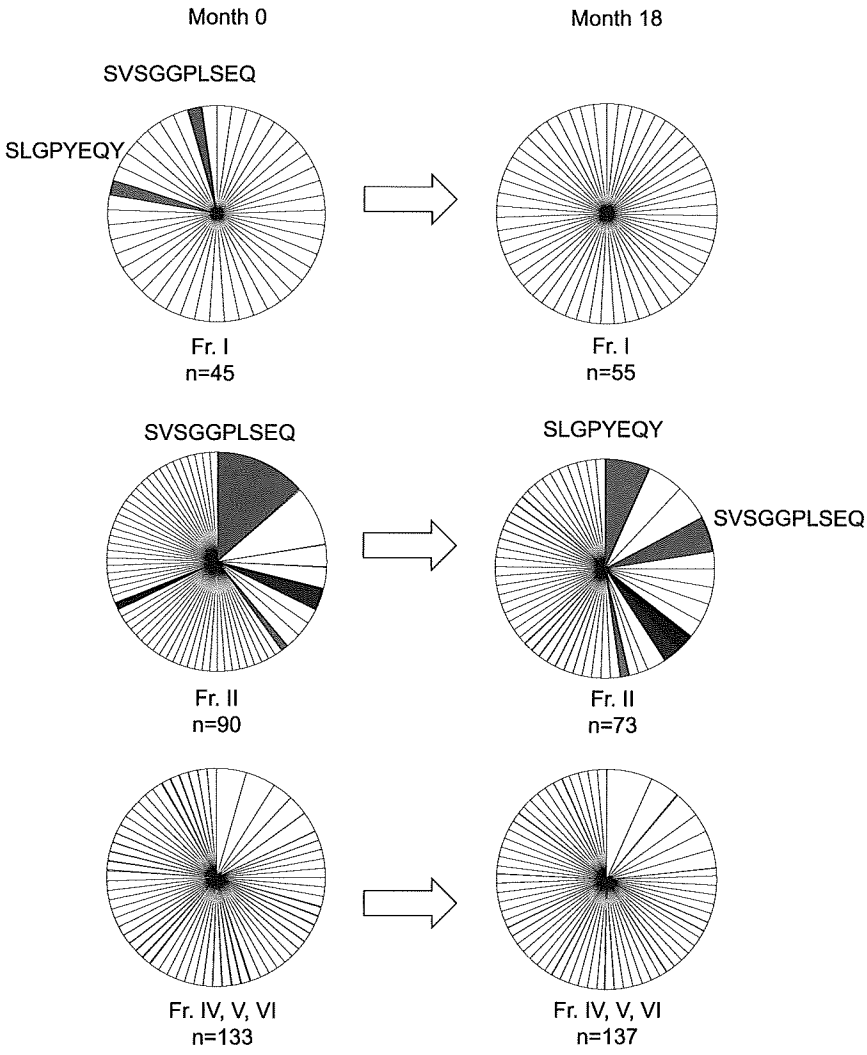

Figure 5. Longitudinal TCR Repertoire Analysis in FoxP3+ Cell Subpopulations

$TCRBV5^+CD4^+$ T cells belonging to indicated Treg or non-Treg cell fractions were FACS sorted as a single cell at indicated time points into wells of PCR plates. By RT-PCR and TCR sequencing, the frequencies of individual sequences were assessed. Empty slices correspond to sequences that were found only once in only one subset. Persistent clones are color highlighted. Slice size is proportional to the number of occurrences of the corresponding TCR sequences. The total number of sequences successfully analyzed in each subset is indicated.

controls signaling thresholds in lymphocytes, hence their state of differentiation and activation (Hermiston et al., 2003). The three subpopulations are $CD45RA^-FoxP3^{hi}CD4^+$ activated Treg cells and $CD45RA^+FoxP3^{lo}CD4^+$ resting Treg cells, both of which are potently suppressive in vitro, and cytokine-secreting nonsuppressive $CD45RA^-FoxP3^{lo}CD4^+$ non-Treg cells.

The distinction of $FoxP3^+$ subpopulations revealed the differentiation pathways of Treg cell subpopulations. First, most of $FoxP3^{hi}$ aTreg cells originate from rTreg cells as shown in vitro and in vivo, although some $FoxP3^{hi}$ Treg cells may arise from $FoxP3^-CD4^+$ non-Treg cells (Vukmanovic-Stejic et al., 2006). Second, a large proportion of $FoxP3^{hi}$ aTreg cells is highly proliferative in vivo and appears to be recently activated, although most rTreg cells are in a resting state. Once rTreg cells are stimulated, they upregulate FoxP3 expression, differentiate to aTreg cells, and proliferate. In addition to these results obtained by direct ex vivo analysis of the subpopulations and by their transfer to NOG mice, our longitudinal study of the repertoire of a particular TCR Vβ subfamily in a single individual provides further evidence that the conversion of rTreg to aTreg cells physiologically occurs in vivo. In our current analysis, dominant clones found in the rTreg cell population were found 18 months later in the aTreg, but not rTreg, cell population. This indicates that the clones have preferentially expanded after differentiating to aTreg cells, as suggested by the high rate of $Ki\text{-}67^+$ cells in the aTreg cell population. The presence of such dominant T cell clones over a long period of time is a key feature of the aTreg cell population (C.P. and G.G., unpublished data). This also indicates that the TCR repertoire of Treg cells adaptively changes with clonal expansion especially in aTreg cells. Considering that aTreg cells rapidly die in vitro and that the immune system is constantly challenged by exogenous and endogenous antigens, it is highly likely that the maintenance of the pool of aTreg cells is the consequence of a tight balance between the constant development of aTreg cells from activated and proliferating rTreg cells and their death after exerting suppression. Further, aTreg cells control rTreg cell expansion in a feedback manner, contributing to the maintenance of the balance. $FoxP3^{hi}$ aTreg cells thus appear to be terminally differentiated Treg cells; yet it remains to be determined whether the aTreg cell population contains a memory type long-living Treg cells. Given that aTreg cells die rapidly and that rTreg cells are highly proliferative upon stimulation, attempts to expand Treg cells ex vivo for cell therapy should be focused on rTreg cells as proposed by others (Hoffmann et al., 2006). It needs to be determined whether rTreg cells are constantly produced by the thymus, or whether they have a high renewal capacity in the periphery, or both.

Our study has clearly shown that human $FoxP3^+CD4^+$ T cells contain cytokine-secreting nonsuppressive effector T cells that display low expression of FoxP3. These nonsuppressive $FoxP3^{lo}CD45RA^-CD4^+$ T cells (Fr. III) may correspond to recently described activation-induced FoxP3-expressing cells that transiently express FoxP3 in vitro (Allan et al., 2007; Gavin et al., 2006; Tran et al., 2007; Wang et al., 2007). Supporting this notion, although the 5′ flanking region of the *FOXP3* gene in $FoxP3^{lo}CD45RA^-CD4^+$ T cells is highly demethylated, the STAT5-responsive region is poorly demethylated, suggesting that they may be unstable in maintaining FoxP3 expression through

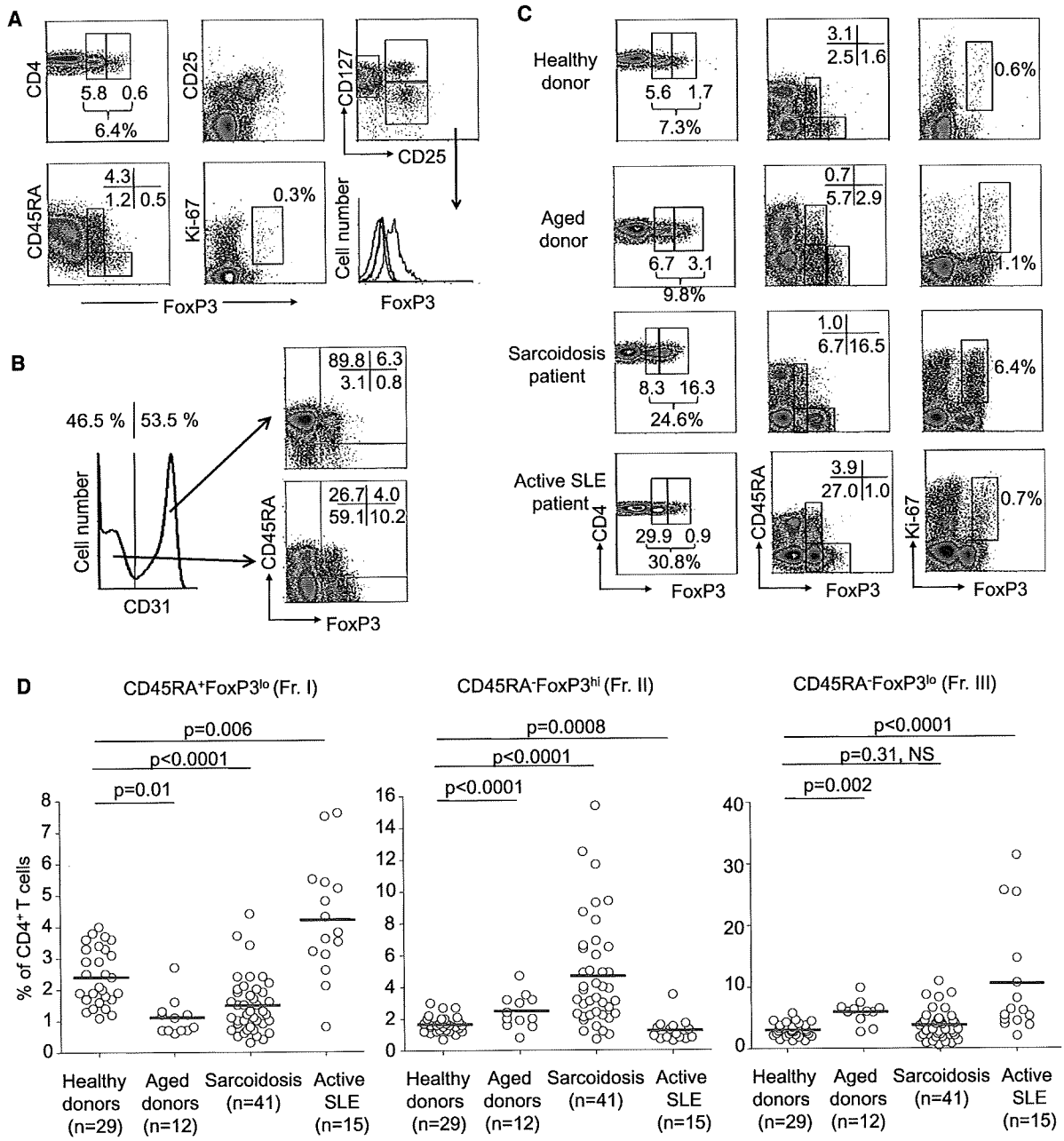

Figure 6. Variations in FoxP3+ Cell Subpopulations under Physiological and Disease Conditions

(A) Flow cytometry of PBMCs gated on $CD4^+$ T cells isolated from cord blood. A representative of four samples.

(B) Expression of CD45RA and FoxP3 by gated $CD31^+$ or $CD31^-$ $CD4^+$ T cells. Numbers indicate percentage in each quadrant. A representative of four independent experiments.

(C) Flow cytometry of PBMCs gated on $CD4^+$ T cells isolated from a 29-year-old healthy adult, an 88-year-old donor, and two patients with active sarcoidosis or active SLE. Percentage of each quadrant in each staining combination is shown.

(D) Percentages of each $FoxP3^+$ subset among $CD4^+$ T cells in indicated numbers of patients with active sarcoidosis, active SLE, aged donors (between 79 and 90 years old), and healthy donors (between 18 and 40 years old). Red horizontal bars represent mean percentage. Statistical comparisons were performed by nonparametric Mann-Whitney U test. NS, not significant.

STAT5 signaling. The notion is also supported by recent reports showing that activation-induced $FoxP3^+CD4^+$ T cells have *FOXP3* DNA significantly less demethylated than bona fide Treg cells (Baron et al., 2007; Janson et al., 2008). In addition, although CD127 is a convenient marker for isolating $FoxP3^+$ cells as $CD25^{hi}CD127^{lo}CD4^+$ T cells (Liu et al., 2006; Seddiki et al., 2006), it is of note that they also include $FoxP3^+$ non-Treg cells. We therefore propose that the combination of CD25 and CD45RA is so far the best markers for purifying human $FoxP3^+$ Treg cells as rTreg and aTreg cells.

We noticed in microarray analysis that RORC, the human ortholog of murine RORγt, a major transcription factor for Th17 cell differentiation (Ivanov et al., 2006), was highly upregulated in both Fr. II and III and much less in Fr. I. Indeed, FoxP3^{lo} memory-like non-Tregs (Fr. III) were the highest producers of IL-17 among CD4$^+$ T cells. These results support recent findings in mice that FoxP3-RORγt double-positive CD4$^+$ T cells can convert into either Treg cells or Th17 cells (Yang et al., 2008a; Zhou et al., 2008). AHR was recently shown in mice to be critical for the differentiation of naive T cells to Th17 versus FoxP3$^+$ Treg cells (Quintana et al., 2008; Veldhoen et al., 2008). Our finding of upregulated AHR repressor in aTreg cells therefore suggests that differentiation of FoxP3$^-$CD4$^+$ T cells to aTreg cells might be regulated through the modulation of AHR activity by AHR repressor. Further study is required to determine how the expression amount of FoxP3 in each FoxP3$^+$ subpopulation contributes to the function of each subset (e.g., suppression and IL-17 production) through interaction with other molecules including RORC.

This study has revealed several key features of Treg cell-mediated suppression in vitro. First, challenging the commonly accepted notion that Treg cells are anergic in vitro, human Treg cells proliferate and die, although the degree of their proliferation is much lower than that of non-Treg cells when Treg cells and non-Treg cells are separately stimulated and compared. Further, the hypoproliferation observed with CD25^{hi}CD4$^+$ T cells can be attributed, in part, to the suppression of rTreg cell proliferation by aTreg cells and also to the death of the latter. These findings mean that thymidine uptake by whole cocultured cells in Treg cell assay may not be accurate to monitor responder cell proliferation in the presence of Treg cells. Second, CTLA-4 expression in aTreg cells, but not in rTreg cells, suggests that aTreg cells are the main effectors of suppression as shown by the fact that Treg cell-specific deficiency impairs Treg cell suppressive function in vivo and in vitro in mice (Wing et al., 2008). Further, FoxP3$^+$ Treg cells out-compete naive T cells in in vitro aggregation around dendritic cells and downregulate their expression of CD80 and CD86 in a CTLA-4-dependent fashion (Onishi et al., 2008). It is likely in humans that, upon activation, rTreg cells differentiate to aTreg cells and exert suppression in vitro through these mechanisms. As another possibility, rTreg and aTreg cells might use different suppressive mechanisms by secreting different immunosuppressive cytokines such as IL-10 and TGF-β (Ito et al., 2008). Our microarray analysis indeed indicates that aTreg cells are more active in IL-10 transcription but less active in TGF-β transcription than rTreg cells. Further study is required to determine whether Treg cells use multiple suppressive mechanisms depending on their differentiation status (Sakaguchi et al., 2008).

Finally, supporting physiological and clinical relevance of distinguishing subpopulations of FoxP3$^+$ T cells, rTreg and aTreg cells can be clearly identified with different proportions in cord blood of healthy newborns, PBL of aged individuals, and patients with SLE or sarcoidosis. In cord blood, we unexpectedly found a small but always detectable population of CD45RA^{lo}Ki-67$^+$FoxP3^{hi}CD4$^+$ T cells that corresponded to adult aTreg cells. This finding suggests that even in fetuses, natural rTreg cells are constantly activated by endogenous self antigens and exogenous antigens derived from maternal circulation. An opposite trend exists in aged donors, who had high proportions of aTreg cells and low but still detectable proportions of rTreg cells. Because of thymus involution observed in aged individuals, one can speculate that, like conventional naive CD4$^+$ T cells (Vrisekoop et al., 2008), rTreg cells can be generated in the periphery in aged individuals to compensate for decreased thymic production of Treg cells; alternatively, but not exclusively, aTreg cells may homeostatically expand to counterbalance the lack of rTreg cells in the periphery. Under pathological conditions, a high prevalence of aTreg cells and a decrease in the rTreg cell population in sarcoidosis suggests that rTreg cells may be swiftly converted into aTreg cells immediately after having emigrated from the thymus or having been peripherally generated. In contrast, in active SLE, the number of aTreg cells decreased while that of rTreg cells remained normal or increased, with a notable increase in FoxP3^{lo}CD4$^+$ non-Treg cells. This also confirms the FoxP3^{lo}CD45RA$^-$ memory/effector-like non-Treg cell subset as a discrete population among FoxP3$^+$ CD4$^+$ T cells. Further functional analysis is required to interpret these anomalies and variations in disease states (Taflin et al., 2009). Yet, analysis of Treg cell function by dissecting FoxP3$^+$ cells into three subpopulations is instrumental for understanding pathophysiology of immunological diseases.

In conclusion, we propose a definition of human FoxP3$^+$ Treg cell subsets based on in vitro and in vivo features of FoxP3-expressing CD4$^+$ T cells. Functional and numerical analysis of each subset will help to understand and control immune responses in normal and disease states.

EXPERIMENTAL PROCEDURES

Human Samples

Blood samples were obtained from young healthy adult volunteers (18–40 years old), from aged control donors (79–90 years old), and from active sarcoidosis or active SLE patients and cord blood samples from full-term neonates who had no hereditary disorders, hematologic abnormalities, or infectious complications. Aged donors had no acute or chronic inflammatory or infectious disease, ongoing thrombosis, or neoplasia. Diagnosis of active SLE and sarcoidosis were made according to previously described criteria (Miyara et al., 2005, 2006). All patients were newly diagnosed and not medicated with steroid or immunosuppressant. The study was done according to the Helsinki declaration with the approval from the human ethics committee of the Institute for Frontier Medical Sciences, Kyoto University and from Comité Consultatif de Protection des Personnes dans la Recherche Biomédicale of Pitié-Salpétrière Hospital, Paris. Human peripheral blood PBMC were prepared by Ficoll gradient centrifugation. Lymphocyte subpopulations was isolated by a MoFLo cell sorter (Dako) after positive magnetic cell separation of CD4$^+$ T cells by CD4$^+$ T cell MACS beads (Miltenyi Biotec). Purity of isolated cells was always >95% (Figure S1). Autologous CD14$^+$ and CD19$^+$ cells positively selected by mixed MACS and irradiated (50 Gy) were used as accessory cells.

Mice

NOG mice described previously (Hiramatsu et al., 2003) were injected intravenously with 3.5–5 × 10^7 human PBMCs. The mice were maintained in our animal facility and treated in accordance with the guidelines of Kyoto University.

Flow Cytometry

Freshly obtained or in vitro cultured lymphocytes and human lymphocytes isolated from NOG mouse spleens were stained with anti-hCD4 (-PerCP-Cy5.5 from BD biosciences or -APC from R&D Systems), anti-hCD25 (-PE or -PE-Cy5 from BD), anti-hCD45RO (-PE from Beckman Coulter and PE-Cy7 from

BD), anti-hCD45RA (-PE-Cy7 from BD or -FITC from Beckman Coulter), anti-ICOS (-FITC from e-Bioscience), anti-HLA-DR (-PE from BD biosciences), anti-CD31 (-APC from e-Bioscience), anti-hCD127 (-PE from Beckman Coulter and -PE-Cy5 from e-bioscience), and 7-AAD (Dako). Intracellular detection of FoxP3 with anti-hFoxP3 (PE or Alexa Fluor 647, clone 236A/E7 [e-Bioscience] or clone 259D [BD biosciences]) and of Ki-67 antigen with Ki-67 antibody (FITC or PE from BD) was performed on fixed and permeabilized cells via Cytofix/Cytoperm (e-Bioscience). For detection of intracellular cytokine production, CD4$^+$ T cells were stimulated with 20 ng/ml PMA and 1 μM ionomycin in the presence of Golgi-Stop (BD Biosciences) for 5 hr and then stained with anti-hFoxP3-PE, Ki-67-FITC, anti-IL2-APC (BD Biosciences), anti-IFN-γ-APC (BD), or anti-IL-17-Alexa Fluor 647 (e-Bioscience) after fixation and permeabilization. Data acquired by FACSCalibur (Becton Dickinson) were analyzed with WinMDI 2.9 software (http://facs.scripps.edu/software.html). Statistical comparisons were performed with the nonparametric Mann-Whitney U test.

Cell Culture and Suppression Assay

RPMI 1640 medium supplemented with 10% fetal bovine serum, 100 IU/ml penicillin, and 100 μg/ml streptomycin (Sigma, St. Louis, MO) was used for T cell culture. Cells were labeled with 1 μM CFSE (Dojindo and Invitrogen). In suppression assays, unless otherwise indicated, 1×10^4 CFSE-labeled responder CD25$^-$CD45RA$^+$CD4$^+$ T cells were cocultured with 1×10^4 unlabeled cells assessed for their suppressive capacity and 1×10^5 irradiated autologous accessory cells and were stimulated with 0.5 μg/mL plate-bound anti-CD3 (OKT3 mAb) in 96-well round-bottom plate in supplemented RPMI medium. Proliferation of CFSE-labeled cells was assessed by flow cytometry after 84–90 hr of culture. Percent suppression was calculated by dividing the number of proliferating CFSE-diluting responder cells in the presence of suppressor cells at a 1 to 1 ratio by the number of proliferating responder cells when cultured alone, and multiplied by 100.

FOXP3 Gene DNA Methylation

The genomic DNA from purified human CD4$^+$ T cell subsets was extracted by the Blood & Tissue Genomic DNA Extraction System (Viogene). Genomic DNA from purified cells was bisulfite converted by the EpiTect Bisulfite Kit (QIAGEN) according to the manufacturer's instructions. DNA was then subjected to PCR with primers for amplification of specific targets in bisulfite-treated DNA. The PCR products obtained were cloned into the pGEM-T Easy vector (Promega) and 20 individual clones from each sample were cycle sequenced by the BigDye Terminator kit (ver. 3.1; Applied Biosystems) and the ABI automated DNA sequencer (Applied Biosystems). Primers used: Fxpro-met_F1, 5′-TTTTT GTGGTGAGGGGAAGAAATTATATT-3′; Fxpro-met_R2, 5′-TACCATCTCCTC CAATAAAACCCACATC-3′; Fxint-met_F8, 5′-TTTGGGTTAAGTTTGTTGTAG GATAGGGTAGTTAG-3′; Fxint-met_R7, 5′-AAATCTACATCTAAACCCTATTAT CACAACCCC-3′.

Single Cell Sorting, RT-PCR, and Vβ5 Sequence Analysis

PBLs were stained with anti-human CD4-FITC, anti-human CD25-PC7 (BD Biosciences), and anti-human BV5.1, BV5.2, BV5.3-PPE (Beckman Coulter). Single cells were sorted with the FACS Vantage (Becton Dickinson) into 96-well PCR plates (Abgene, Epsom). Single-cell RT-PCR conditions were as previously described (Miyara et al., 2006). In the first PCR round, BV5ext (5′-GATCAAAACGAGAGGACAGC-3′) and BC (5′-CGGGCTGCTCCTTGAG GGGCTGCG-3′) were used. Reactions were subjected after 5 min at 94°C to 8 cycles (94°C for 30 s, 60°C for 40 s, 72°C for 50 s), 32 cycles (94°C for 30 s, 55°C for 40 s, 72°C for 50 s), and a final elongation at 72°C for 5 min. In a second PCR round, nested primers BV5 (5′-AGCTCTGAGCTGAATGT GAACGCC-3′) and BC-int (5′-GCGGGTCYGTGCTGACCC-3′) were used. PCR was performed as in the first step.

Products were subjected to automated sequencing (ABI 3100, Applied Biosystems).

Specific questions regarding this repertoire analysis should be sent to guy.gorochov@upmc.fr.

Microarray and Real-Time PCR

RNA was extracted from FACS-sorted CD4$^+$ T cells according to their amounts of CD25 and CD45RA and analyzed by Affymetrix Human Genome U133 Plus 2.0 Arrays.

Real-time PCR was performed with a SYBR green assay on the LightCycler 480 system (Roche). Total RNA extracted from FACS-sorted T cells was reverse transcribed according to the manufacturer's instructions (RNeasy Micro kit, QIAGEN). In each reaction, hypoxanthine phosphoribosyltransferase-1 (HPRT-1) was amplified as a housekeeping gene to calculate a standard curve and to correct for variations in target sample quantities. Relative copy numbers were calculated for each sample from the standard curve after normalization to HPRT-1 by the instrument software. Primers used: FOXP3_F, 5′- CAGCACATTCCCAGAGTTCC-3′; FOXP3_R,5′-TGAGCGTGGCGTAGGT GAAAG-3′; RORA_F,5′- TCACCAACGGCGAGACTTC-3′; RORA_R,5′-GGCA AACTCCACCACATACTG-3′; RORC_F,5′-CGCTCCAACATCTTCTCC-3′; RO RC_R,5′-CTAACCAGCACCACTTCC-3′; AHR_F,5′-AACAGATGAGGAAGGAA CAGAGC-3′; AHR_R,5′-GAGTGGATGTGGTAGCAGAGTC-3′; AHRR_F,5′- AA GGCTGCTGTTGGAGTC-3′; AHRR_R,5′- TGGATGTAGTCATAAATGTTCTG G-3′; HPRT-1_F,5′-GCTGAGGATTTGGAAAGGGTG-3′; HPRT-1_R,5′-TGAG CACACAGAGGGCTACAATG-3′.

ACCESSION NUMBERS

Microarray data are available from the National Center for Biotechnology Information Gene Expression Omnibus (GEO) under accession number GSE15659.

SUPPLEMENTAL DATA

Supplemental Data include ten figures and two tables and can be found with this article online at http://www.cell.com/immunity/supplemental/S1074-7613(09)00202-7.

ACKNOWLEDGMENTS

This work was supported by grant in aid from the Ministry of Education, Sports, and Culture of Japan. M.M. was successively supported by la Fondation pour la Recherche Médicale and by Japan Society for the Promotion of Science. The study was also in part supported by a grant from the European Union (ATTACK project LHS-CT-2005-018914). We thank the blood donors and the patients who participated in the study, R. Ishii for expertise in cell sorting, M. Kakino for assistance in molecular biology, M. Yoshida for maintaining mice, and S. Teradaira, A. Kishi, M. Hashimoto, S. Maeda, H. Uryu, K. Hirota, C. Badoual, and N. Sakaguchi for technical help and valuable discussion.

Received: December 25, 2008
Revised: February 23, 2009
Accepted: March 26, 2009
Published online: May 21, 2009

REFERENCES

Allan, S.E., Crome, S.Q., Crellin, N.K., Passerini, L., Steiner, T.S., Bacchetta, R., Roncarolo, M.G., and Levings, M.K. (2007). Activation-induced FOXP3 in human T effector cells does not suppress proliferation or cytokine production. Int. Immunol. *19*, 345–354.

Baecher-Allan, C., Brown, J.A., Freeman, G.J., and Hafler, D.A. (2001). CD4+CD25high regulatory cells in human peripheral blood. J. Immunol. *167*, 1245–1253.

Baecher-Allan, C., Wolf, E., and Hafler, D.A. (2006). MHC class II expression identifies functionally distinct human regulatory T cells. J. Immunol. *176*, 4622–4631.

Baron, U., Floess, S., Wieczorek, G., Baumann, K., Grutzkau, A., Dong, J., Thiel, A., Boeld, T.J., Hoffmann, P., Edinger, M., et al. (2007). DNA demethylation in the human FOXP3 locus discriminates regulatory T cells from activated FOXP3(+) conventional T cells. Eur. J. Immunol. *37*, 2378–2389.

Curiel, T.J., Coukos, G., Zou, L., Alvarez, X., Cheng, P., Mottram, P., Evdemon-Hogan, M., Conejo-Garcia, J.R., Zhang, L., Burow, M., et al. (2004). Specific recruitment of regulatory T cells in ovarian carcinoma fosters immune privilege and predicts reduced survival. Nat. Med. *10*, 942–949.

Dieckmann, D., Plottner, H., Berchtold, S., Berger, T., and Schuler, G. (2001). Ex vivo isolation and characterization of CD4(+)CD25(+) T cells with regulatory properties from human blood. J. Exp. Med. *193*, 1303–1310.

Ehrenstein, M.R., Evans, J.G., Singh, A., Moore, S., Warnes, G., Isenberg, D.A., and Mauri, C. (2004). Compromised function of regulatory T cells in rheumatoid arthritis and reversal by anti-TNFalpha therapy. J. Exp. Med. *200*, 277–285.

Floess, S., Freyer, J., Siewert, C., Baron, U., Olek, S., Polansky, J., Schlawe, K., Chang, H.D., Bopp, T., Schmitt, E., et al. (2007). Epigenetic control of the foxp3 locus in regulatory T cells. PLoS Biol. *5*, e38.

Fontenot, J.D., Gavin, M.A., and Rudensky, A.Y. (2003). Foxp3 programs the development and function of CD4+CD25+ regulatory T cells. Nat. Immunol. *4*, 330–336.

Fritzsching, B., Oberle, N., Pauly, E., Geffers, R., Buer, J., Poschl, J., Krammer, P., Linderkamp, O., and Suri-Payer, E. (2006). Naive regulatory T cells: A novel subpopulation defined by resistance toward CD95L-mediated cell death. Blood *108*, 3371–3378.

Gavin, M.A., Torgerson, T.R., Houston, E., DeRoos, P., Ho, W.Y., Stray-Pedersen, A., Ocheltree, E.L., Greenberg, P.D., Ochs, H.D., and Rudensky, A.Y. (2006). Single-cell analysis of normal and FOXP3-mutant human T cells: FOXP3 expression without regulatory T cell development. Proc. Natl. Acad. Sci. USA *103*, 6659–6664.

Hermiston, M.L., Xu, Z., and Weiss, A. (2003). CD45: A critical regulator of signaling thresholds in immune cells. Annu. Rev. Immunol. *21*, 107–137.

Hiramatsu, H., Nishikomori, R., Heike, T., Ito, M., Kobayashi, K., Katamura, K., and Nakahata, T. (2003). Complete reconstitution of human lymphocytes from cord blood CD34+ cells using the NOD/SCID/gammacnull mice model. Blood *102*, 873–880.

Hoffmann, P., Eder, R., Boeld, T.J., Doser, K., Piseshka, B., Andreesen, R., and Edinger, M. (2006). Only the CD45RA+ subpopulation of CD4+CD25high T cells gives rise to homogeneous regulatory T-cell lines upon in vitro expansion. Blood *108*, 4260–4267.

Hori, S., Nomura, T., and Sakaguchi, S. (2003). Control of regulatory T cell development by the transcription factor Foxp3. Science *299*, 1057–1061.

Ito, T., Hanabuchi, S., Wang, Y.H., Park, W.R., Arima, K., Bover, L., Qin, F.X., Gilliet, M., and Liu, Y.J. (2008). Two functional subsets of FOXP3+ regulatory T cells in human thymus and periphery. Immunity *28*, 870–880.

Ivanov, I.I., McKenzie, B.S., Zhou, L., Tadokoro, C.E., Lepelley, A., Lafaille, J.J., Cua, D.J., and Littman, D.R. (2006). The orphan nuclear receptor RORgammat directs the differentiation program of proinflammatory IL-17+ T helper cells. Cell *126*, 1121–1133.

Janson, P.C., Winerdal, M.E., Marits, P., Thorn, M., Ohlsson, R., and Winqvist, O. (2008). FOXP3 promoter demethylation reveals the committed Treg population in humans. PLoS ONE *3*, e1612.

Jonuleit, H., Schmitt, E., Stassen, M., Tuettenberg, A., Knop, J., and Enk, A.H. (2001). Identification and functional characterization of human CD4(+)CD25(+) T cells with regulatory properties isolated from peripheral blood. J. Exp. Med. *193*, 1285–1294.

Khattri, R., Cox, T., Yasayko, S.A., and Ramsdell, F. (2003). An essential role for Scurfin in CD4+CD25+ T regulatory cells. Nat. Immunol. *4*, 337–342.

Kimmig, S., Przybylski, G.K., Schmidt, C.A., Laurisch, K., Mowes, B., Radbruch, A., and Thiel, A. (2002). Two subsets of naive T helper cells with distinct T cell receptor excision circle content in human adult peripheral blood. J. Exp. Med. *195*, 789–794.

Kriegel, M.A., Lohmann, T., Gabler, C., Blank, N., Kalden, J.R., and Lorenz, H.M. (2004). Defective suppressor function of human CD4+ CD25+ regulatory T cells in autoimmune polyglandular syndrome type II. J. Exp. Med. *199*, 1285–1291.

Levings, M.K., Sangregorio, R., and Roncarolo, M.G. (2001). Human cd25(+)cd4(+) t regulatory cells suppress naive and memory T cell proliferation and can be expanded in vitro without loss of function. J. Exp. Med. *193*, 1295–1302.

Liu, W., Putnam, A.L., Xu-Yu, Z., Szot, G.L., Lee, M.R., Zhu, S., Gottlieb, P.A., Kapranov, P., Gingeras, T.R., Fazekas de St Groth, B., et al. (2006). CD127 expression inversely correlates with FoxP3 and suppressive function of human CD4+ T reg cells. J. Exp. Med. *203*, 1701–1711.

Mantel, P.Y., Ouaked, N., Ruckert, B., Karagiannidis, C., Welz, R., Blaser, K., and Schmidt-Weber, C.B. (2006). Molecular mechanisms underlying FOXP3 induction in human T cells. J. Immunol. *176*, 3593–3602.

Miyara, M., Amoura, Z., Parizot, C., Badoual, C., Dorgham, K., Trad, S., Nochy, D., Debre, P., Piette, J.C., and Gorochov, G. (2005). Global natural regulatory T cell depletion in active systemic lupus erythematosus. J. Immunol. *175*, 8392–8400.

Miyara, M., Amoura, Z., Parizot, C., Badoual, C., Dorgham, K., Trad, S., Kambouchner, M., Valeyre, D., Chapelon-Abric, C., Debre, P., et al. (2006). The immune paradox of sarcoidosis and regulatory T cells. J. Exp. Med. *203*, 359–370.

Ng, W.F., Duggan, P.J., Ponchel, F., Matarese, G., Lombardi, G., Edwards, A.D., Isaacs, J.D., and Lechler, R.I. (2001). Human CD4(+)CD25(+) cells: a naturally occurring population of regulatory T cells. Blood *98*, 2736–2744.

Onishi, Y., Fehervari, Z., Yamaguchi, T., and Sakaguchi, S. (2008). Foxp3+ natural regulatory T cells preferentially form aggregates on dendritic cells in vitro and actively inhibit their maturation. Proc. Natl. Acad. Sci. USA *105*, 10113–10118.

Quintana, F.J., Basso, A.S., Iglesias, A.H., Korn, T., Farez, M.F., Bettelli, E., Caccamo, M., Oukka, M., and Weiner, H.L. (2008). Control of T(reg) and T(H)17 cell differentiation by the aryl hydrocarbon receptor. Nature *453*, 65–71.

Roncador, G., Brown, P.J., Maestre, L., Hue, S., Martinez-Torrecuadrada, J.L., Ling, K.L., Pratap, S., Toms, C., Fox, B.C., Cerundolo, V., et al. (2005). Analysis of FOXP3 protein expression in human CD4+CD25+ regulatory T cells at the single-cell level. Eur. J. Immunol. *35*, 1681–1691.

Sakaguchi, S., Sakaguchi, N., Asano, M., Itoh, M., and Toda, M. (1995). Immunologic self-tolerance maintained by activated T cells expressing IL-2 receptor alpha-chains (CD25). Breakdown of a single mechanism of self-tolerance causes various autoimmune diseases. J. Immunol. *155*, 1151–1164.

Sakaguchi, S., Yamaguchi, T., Nomura, T., and Ono, M. (2008). Regulatory T cells and immune tolerance. Cell *133*, 775–787.

Seddiki, N., Santner-Nanan, B., Martinson, J., Zaunders, J., Sasson, S., Landay, A., Solomon, M., Selby, W., Alexander, S.I., Nanan, R., et al. (2006). Expression of interleukin (IL)-2 and IL-7 receptors discriminates between human regulatory and activated T cells. J. Exp. Med. *203*, 1693–1700.

Taams, L.S., Smith, J., Rustin, M.H., Salmon, M., Poulter, L.W., and Akbar, A.N. (2001). Human anergic/suppressive CD4(+)CD25(+) T cells: a highly differentiated and apoptosis-prone population. Eur. J. Immunol. *31*, 1122–1131.

Taflin, C., Miyara, M., Nochy, D., Valeyre, D., Naccache, J.M., Altare, F., Salek-Peyron, P., Badoual, C., Bruneval, P., Haroche, J., et al. (2009). FoxP3+ regulatory T cells suppress early stages of granuloma formation but have little impact on sarcoidosis lesions. Am. J. Pathol. *174*, 497–508.

Tran, D.Q., Ramsey, H., and Shevach, E.M. (2007). Induction of FOXP3 expression in naive human CD4+FOXP3 T cells by T-cell receptor stimulation is transforming growth factor-{beta} dependent but does not confer a regulatory phenotype. Blood *110*, 2983–2990.

Valmori, D., Merlo, A., Souleimanian, N.E., Hesdorffer, C.S., and Ayyoub, M. (2005). A peripheral circulating compartment of natural naive CD4 Tregs. J. Clin. Invest. *115*, 1953–1962.

Veldhoen, M., Hirota, K., Westendorf, A.M., Buer, J., Dumoutier, L., Renauld, J.C., and Stockinger, B. (2008). The aryl hydrocarbon receptor links T(H)17-cell-mediated autoimmunity to environmental toxins. Nature *453*, 106–109.

Viglietta, V., Baecher-Allan, C., Weiner, H.L., and Hafler, D.A. (2004). Loss of functional suppression by CD4+CD25+ regulatory T cells in patients with multiple sclerosis. J. Exp. Med. *199*, 971–979.

Vrisekoop, N., den Braber, I., de Boer, A.B., Ruiter, A.F., Ackermans, M.T., van der Crabben, S.N., Schrijver, E.H., Spierenburg, G., Sauerwein, H.P., Hazenberg, M.D., et al. (2008). Sparse production but preferential incorporation of recently produced naive T cells in the human peripheral pool. Proc. Natl. Acad. Sci. USA *105*, 6115–6120.

Vukmanovic-Stejic, M., Zhang, Y., Cook, J.E., Fletcher, J.M., McQuaid, A., Masters, J.E., Rustin, M.H., Taams, L.S., Beverley, P.C., Macallan, D.C., and

Akbar, A.N. (2006). Human CD4+ CD25hi Foxp3+ regulatory T cells are derived by rapid turnover of memory populations in vivo. J. Clin. Invest. *116*, 2423–2433.

Wang, J., Ioan-Facsinay, A., van der Voort, E.I., Huizinga, T.W., and Toes, R.E. (2007). Transient expression of FOXP3 in human activated nonregulatory CD4+ T cells. Eur. J. Immunol. *37*, 129–138.

Wing, K., Onishi, Y., Prieto-Martin, P., Yamaguchi, T., Miyara, M., Fehervari, Z., Nomura, T., and Sakaguchi, S. (2008). CTLA-4 control over Foxp3+ regulatory T cell function. Science *322*, 271–275.

Yagi, H., Nomura, T., Nakamura, K., Yamazaki, S., Kitawaki, T., Hori, S., Maeda, M., Onodera, M., Uchiyama, T., Fujii, S., and Sakaguchi, S. (2004). Crucial role of FOXP3 in the development and function of human CD25+CD4+ regulatory T cells. Int. Immunol. *16*, 1643–1656.

Yang, X.O., Nurieva, R., Martinez, G.J., Kang, H.S., Chung, Y., Pappu, B.P., Shah, B., Chang, S.H., Schluns, K.S., Watowich, S.S., et al. (2008a). Molecular antagonism and plasticity of regulatory and inflammatory T cell programs. Immunity *29*, 44–56.

Yang, X.O., Pappu, B.P., Nurieva, R., Akimzhanov, A., Kang, H.S., Chung, Y., Ma, L., Shah, B., Panopoulos, A.D., Schluns, K.S., et al. (2008b). T helper 17 lineage differentiation is programmed by orphan nuclear receptors ROR alpha and ROR gamma. Immunity *28*, 29–39.

Zhou, L., Lopes, J.E., Chong, M.M., Ivanov, I.I., Min, R., Victora, G.D., Shen, Y., Du, J., Rubtsov, Y.P., Rudensky, A.Y., et al. (2008). TGF-beta-induced Foxp3 inhibits T(H)17 cell differentiation by antagonizing RORgammat function. Nature *453*, 236–240.

Zorn, E., Nelson, E.A., Mohseni, M., Porcheray, F., Kim, H., Litsa, D., Bellucci, R., Raderschall, E., Canning, C., Soiffer, R.J., et al. (2006). IL-2 regulates FOXP3 expression in human CD4+CD25+ regulatory T cells through a STAT-dependent mechanism and induces the expansion of these cells in vivo. Blood *108*, 1571–1579.

copy number in TG of $GrB^{-/-}$ or $Pfn^{-/-}$ mice. This mechanism might be particularly efficient during attempted HSV-1 reactivation events where ICP4 expression has escaped repression by viral miRNAs and host neuron epigenetic modifications. Thus, we propose a tripartite relation in which HSV-1 latency is maintained through the activity of the virus, host neuron, and contiguous $CD8^+$ T cells permitting viral persistence with neuronal survival (fig. S7).

References and Notes

1. D. Theil *et al.*, *Am. J. Pathol.* **163**, 2179 (2003).
2. K. Hufner *et al.*, *J. Neuropathol. Exp. Neurol.* **65**, 1022 (2006).
3. G. M. Verjans *et al.*, *Proc. Natl. Acad. Sci. U.S.A.* **104**, 3496 (2007).
4. T. Derfuss *et al.*, *Brain Pathol.* **17**, 389 (2007).
5. A. Simmons, D. C. Tscharke, *J. Exp. Med.* **175**, 1337 (1992).
6. E. M. Cantin, D. R. Hinton, J. Chen, H. Openshaw, *J. Virol.* **69**, 4898 (1995).
7. C. Shimeld *et al.*, *J. Neuroimmunol.* **61**, 7 (1995).
8. T. Liu, Q. Tang, R. L. Hendricks, *J. Virol.* **70**, 264 (1996).
9. K. M. Khanna, R. H. Bonneau, P. R. Kinchington, R. L. Hendricks, *Immunity* **18**, 593 (2003).
10. T. Liu *et al.*, *J. Exp. Med.* **191**, 1459 (2000).
11. M. L. Freeman, B. S. Sheridan, R. H. Bonneau, R. L. Hendricks, *J. Immunol.* **179**, 322 (2007).
12. K. D. Croen *et al.*, *N. Engl. J. Med.* **317**, 1427 (1987).
13. W. G. Stroop, D. C. Schaefer, *Acta Neuropathol.* **74**, 124 (1987).
14. T. Liu, K. M. Khanna, B. N. Carriere, R. L. Hendricks, *J. Virol.* **75**, 11178 (2001).
15. V. Decman, P. R. Kinchington, S. A. Harvey, R. L. Hendricks, *J. Virol.* **79**, 10339 (2005).
16. Materials and methods are available as supporting material on *Science* Online.
17. W. G. Telford, A. Komoriya, B. Z. Packard, *Cytometry* **47**, 81 (2002).
18. G.-C. Perng *et al.*, *Science* **287**, 1500 (2000).
19. Y. Hoshino, L. Pesnicak, J. I. Cohen, S. E. Straus, *J. Virol.* **81**, 8157 (2007).
20. R. A. Pereira, M. M. Simon, A. Simmons, *J. Virol.* **74**, 1029 (2000).
21. F. Andrade *et al.*, *EMBO J.* **26**, 2148 (2007).
22. C. Backes *et al.*, *Nucleic Acids Res.* **33**, W208 (2005).
23. N. A. DeLuca, A. M. McCarthy, P. A. Schaffer, *J. Virol.* **56**, 558 (1985).
24. J. L. Umbach *et al.*, *Nature* **454**, 780 (2008).
25. D. M. Knipe, A. Cliffe, *Nat. Rev. Microbiol.* **6**, 211 (2008).
26. B. S. Sheridan, J. E. Knickelbein, R. L. Hendricks, *Expert Opin. Biol. Ther.* **7**, 1323 (2007).
27. S. N. Mueller *et al.*, *J. Virol.* **77**, 2445 (2003).

28. We thank K. Lathrop and J. Karlsson for assistance with microscopy and preparation of figures and N. Zurowski for assistance with flow cytometry. We have no conflicting financial interests. This work was supported by NIH grants F30NS061471 (J.E.K.), R01EY05945 (R.L.H.), R01EY015291 (P.R.K.), and P30EY08098 (R.L.H.); a Research to Prevent Blindness Medical Student Eye Research Fellowship (J.E.K.); and unrestricted grants from Research to Prevent Blindness and the Eye and Ear Foundation of Pittsburgh (R.L.H.).

Supporting Online Material

www.sciencemag.org/cgi/content/full/322/5899/268/DC1
Materials and Methods
Figs. S1 to S7
References

4 August 2008; accepted 11 September 2008
10.1126/science.1164164

CTLA-4 Control over Foxp3$^+$ Regulatory T Cell Function

Kajsa Wing,[1]* Yasushi Onishi,[1,2] Paz Prieto-Martin,[1] Tomoyuki Yamaguchi,[1] Makoto Miyara,[1] Zoltan Fehervari,[1] Takashi Nomura,[1] Shimon Sakaguchi[1,3,4]†

Naturally occurring Foxp3$^+$CD4$^+$ regulatory T cells (Tregs) are essential for maintaining immunological self-tolerance and immune homeostasis. Here, we show that a specific deficiency of cytotoxic T lymphocyte antigen 4 (CTLA-4) in Tregs results in spontaneous development of systemic lymphoproliferation, fatal T cell–mediated autoimmune disease, and hyperproduction of immunoglobulin E in mice, and it also produces potent tumor immunity. Treg-specific CTLA-4 deficiency impairs in vivo and in vitro suppressive function of Tregs—in particular, Treg-mediated down-regulation of CD80 and CD86 expression on dendritic cells. Thus, natural Tregs may critically require CTLA-4 to suppress immune responses by affecting the potency of antigen-presenting cells to activate other T cells.

Naturally occurring $CD25^+CD4^+$ regulatory T cells (Tregs), which specifically express the transcription factor Foxp3, suppress aberrant immune responses, including autoimmune diseases and allergy (*1*). Furthermore, reduction or expansion of Tregs can be exploited to provoke effective tumor immunity or transplantation tolerance, respectively. Two cardinal features of Foxp3$^+$ Tregs are that they constitutively express cytotoxic T lymphocyte antigen 4 (CTLA-4), which only happens after activation in other T cell subsets (*2*–*4*), and that Foxp3 controls the expression of CTLA-4 in Tregs (*5*–*9*). CTLA-4 is a potent negative regulator of T cell immune responses, as illustrated by CTLA-4 knockout (KO) mice, which die prematurely from multiorgan inflammation (*10*, *11*). The polymorphism of the CTLA-4 gene contributes substantially to the genetic susceptibility to autoimmune diseases such as type 1 diabetes (*12*). Moreover, autoimmunity, inflammatory bowel disease, and tumor immunity can be elicited by blocking CTLA-4 with a specific antibody (*3*, *4*, *13*–*15*). Yet the manner in which CTLA-4 negatively controls immune responses is controversial (*16*). CTLA-4 expressed by activated effector T cells may mediate a negative signal that attenuates their activation. Alternatively, but not exclusively, Foxp3$^+$ Tregs may require CTLA-4 for their suppressive function. By specifically deleting the CTLA-4 gene in Foxp3$^+$ Tregs in mice, we have attempted to determine the role of CTLA-4 for the maintenance of self-tolerance and immune homeostasis.

We generated BALB/c mice expressing Cre under the control of the Foxp3 promoter—hereafter called FIC (Fox-IRES-Cre) mice—and BALB/c mice expressing a floxed CTLA-4 gene (CTLA-$4^{fl/fl}$) [supporting online material (SOM) text and fig. S1] (*17*). Compared with BALB/c wild-type (WT) mice, FIC mice expressed Foxp3 protein at slightly lower levels whereas CTLA-$4^{fl/fl}$ mice expressed equivalent levels of CTLA-4 (Fig. 1A). To assess the specificity of Cre expression, FIC mice were crossed with Cre reporter mice (CAG mice), which express enhanced green fluorescent protein (EGFP) only in Cre^+ cells (*18*). EGFP expression was confined to ~15% of $CD4^+$ T cells and ~1.5% of $CD8^+$ T cells (Fig. 1B). The vast majority of $EGFP^+CD4^+$ T cells in adult $FIC^{+/+}$ CAG mice were $Foxp3^+$ ($97.1 \pm 1.2\%$, $n = 4$ mice), indicating that Foxp3 expression is stable once the gene is turned on and Cre expression is not leaky in $Foxp3^-$ cells (Fig. 1C). On the basis of this specific expression of Cre in Foxp3$^+$ Tregs, we generated CTLA-4 conditional KO (CKO) mice by crossing FIC and CTLA-$4^{fl/fl}$ mice. CTLA-4 was specifically deleted in $CD4^+Foxp3^+$ T cells, as compared with $FIC^{+/+}$ WT or full CTLA-4 KO mice (Fig. 1D). CKO mice even harbored a higher frequency of CTLA-4–expressing $CD4^+Foxp3^-$ cells than did WT littermates (Fig. 1E). Whereas KO mice became moribund at ~20 days of age (*10*, *11*), CKO mice remained apparently unaffected until ~7 weeks of age, when they rapidly became inactive and began to develop general edema that was frequently accompanied by ascites (Fig. 1F). Thus, CTLA-4 deficiency in Tregs alone suffices to cause fatal disease, whereas the additional CTLA-4 deficiency in non-Treg cells enhances the disease. Yet, CTLA-4 expression in activated effector T cells per se is insufficient to prevent it.

Pathological analysis of CKO mice revealed splenomegaly and lymphadenopathy, which was reflected in increased cell numbers (Fig. 2, A and B). The proportion of $CD4^+$ T cells was unaltered, whereas $CD8^+$ T cells were decreased (Fig. 2C). Cardiomegaly and congestion of the liver was macroscopically evident in the terminal stage of every case. In affected hearts, mononuclear cells densely infiltrated into the myocardium and destroyed myocytes (Fig. 2, D to G), indicating that the plausible cause of sudden death in CKO mice is

[1]Department of Experimental Pathology, Institute for Frontier Medical Sciences, Kyoto University, Kyoto 606-8507, Japan. [2]Department of Rheumatology and Haematology, Tohoku University Graduate School of Medicine, Sendai 980-8574, Japan. [3]Core Research for Evolutional Science and Technology, Japan Science and Technology Agency, Kawaguchi 332-0012, Japan. [4]Laboratory of Experimental Immunology, World Premier International Immunology Frontier Research Center, Osaka University, Suita 565-0871, Japan.

*Present address: Department of Medical Inflammation Research, Karolinska Institute, Stockholm 17177, Sweden.
†To whom correspondence should be addressed. E-mail: shimon@frontier.kyoto-u.ac.jp

heart failure due to severe myocarditis (*19*). In addition, CKO mice possessed focal lymphocyte infiltrations in lung and salivary gland and suffered from gastritis with various degrees of destruction of gastric parietal cells and chief cells. Antiparietal autoantibodies were readily detected in the sera of CKO mice and a proportion of $FIC^{+/+}$ mice, in which the lower expression of Foxp3 in Tregs (Fig. 1A) might somehow affect Treg function (*20*) (Fig. 2, H to N, and SOM text). Myocarditis and gastritis in CKO mice (and gastritis in FIC mice) could be adoptively transferred with splenocytes and purified $CD4^+$ T cells into T cell–deficient BALB/c athymic nude (nu/nu) mice, indicating that these autoimmune conditions were both T cell–mediated (Fig. 2O and fig. S2). Furthermore, CKO mice developed several hundred–fold and threefold higher levels of serum immunoglobulin E (IgE) and immunoglobulin G (IgG), respectively, than the levels in FIC or WT mice (Fig. 2, P and Q).

Costaining of intracellular cytokines and Foxp3 revealed an increased frequency of interleukin-2 (IL-2)–, IL-4–, and IFN-γ–producing $Foxp3^-CD4^+$ cells in both the spleen and lymph node (LN) of diseased CKO and KO mice (Fig. 2R and fig. S3). IL-17–secreting (Th17) cells increased in KO but not CKO mice, suggesting that Th17 cells might contribute to the rapid disease progression in the former. Thus, CTLA-4–deficient Tregs fail to control the spontaneous activation of other T cells and their differentiation into Th1 and Th2 lineage cells that mediate autoimmune disease and allergy.

We next tested whether Treg-specific CTLA-4 deficiency also influenced the potency of tumor immunity. BALB/c nu/nu mice were reconstituted with splenocytes from CKO or control FIC mice containing equivalent numbers of T cells and inoculated with BALB/c-derived RL♂1 leukemia cells (*21*). All recipients of FIC splenocytes died of tumor progression within a month. In contrast, recipients of CKO splenocytes halted the tumor growth, with the majority surviving the 6-week observation period, during which 60% of them completely rejected the tumor (Fig. 3A). As previously shown (*21*), transfer of BALB/c splenocytes after depletion of $CD25^+$ T cells led to the rejection of RL♂1 leukemia cells in nu/nu mice. In this setting, FIC Tregs cotransferred with $CD25^-$ T cells suppressed tumor rejection, whereas CKO Tregs did not (Fig. 3B). Thus, Treg-specific CTLA-4 deficiency affects in vivo Treg suppressive function, leading to enhanced tumor immunity.

We next explored the possibility that CTLA-4 deficiency might impair the generation, survival, or suppressive function of $Foxp3^+$ Tregs. CKO mice exhibited no significant alteration in number or composition of $CD4^+$ and $CD8^+$ thymocytes (Fig. 4A). The majority of $Foxp3^+$ WT thymocytes expressed CTLA-4, whereas $Foxp3^+$ CKO thymocytes contained a mix of $CTLA\text{-}4^+$ and $CTLA\text{-}4^-$ cells in both the CD4–single positive and CD4/CD8–double positive compartments (Fig. 4A). Because the CTLA-4 gene is deleted only after Foxp3 is expressed, CTLA-4 is either up-regulated before Foxp3 expression in CKO mice or it may take some time for the Cre protein to accumulate in $Foxp3^+$ cells, meanwhile allowing the expression of CTLA-4. The frequency of $Foxp3^+$ thymocytes was not significantly changed between CKO and WT mice, whereas the number of $Foxp3^+$ and $Foxp3^-$ T cells in the spleen and LNs increased enormously by active proliferation (Fig. 4B, figs. S4 and S5, and SOM text). Thus, Foxp3-inducible CTLA-4 deficiency minimally alters thymic selection of Tregs and probably triggers immunological diseases through affecting Treg function in the periphery.

Because Foxp3 is encoded by the X chromosome, female nonautoimmune $FIC^{+/-}CTLA\text{-}4^{fl/fl}$ mice are a mosaic for CTLA-4–intact and –deficient Tregs. They harbored equal numbers of $CTLA\text{-}4^+$ and $CTLA\text{-}4^-$ $Foxp3^+$ T cells, indicating that both populations equally survive in physiological non-inflammatory conditions (Fig. 4C). Furthermore, when CTLA-4–deficient or –intact Tregs were transferred to nu/nu mice, both populations showed a similar degree of homeostatic proliferation, and neither one caused autoimmunity (fig. S6). CTLA-4–deficient $Foxp3^+$ Tregs were as poor at producing pro-inflammatory cytokines as were their WT or FIC counterparts (fig. S3). Taken together, CTLA-4 deficiency, per se, does not affect the survival of Tregs or render them pathogenic.

Phenotypically, CTLA-4–deficient naive Tregs in $FIC^{+/-}CTLA\text{-}4^{fl/fl}$ females normally expressed typical Treg markers including CD44, CD103, glucocorticoid-induced tumor necrosis factor receptor, latency-associated peptide, and intracellular IL-10 (Fig. 4D and fig. S7). The comparatively higher expression of these molecules by Tregs from CKO mice is presumably secondary to ongoing inflammation in CKO mice, as illustrated by an activated phenotype of their $Foxp3^-$ non-Treg cells.

CTLA-4–deficient Tregs, whether naive from $FIC^{+/-}CTLA\text{-}4^{fl/fl}$ CAG females or activated from CKO mice, had diminished suppressive capacity compared with CTLA-4–intact Tregs in cultures of carboxyfluorescein diacetate succinimidyl ester (CFSE)–labeled responder T cells (Tresp) in the presence of splenic $CD11c^+$ dendritic cells (DCs) and anti-CD3 monoclonal antibody (mAb), as assessed by the percentage and number of CFSE-diluting (i.e., divided) Tresp (Fig. 4E, figs. S8 and S9, and SOM text). Moreover, CKO Tregs clearly failed to suppress allo-reactive Tresp proliferation, even at high Treg/Tresp ratios (Fig. 4F). FIC or WT Tregs, whether cultured alone or together with Tresp cells, specifically hampered up-regulation of the expression of CD80 and CD86, but not CD40 and major histocompatability complex class II, in DCs (*22*–*26*). In contrast, CKO Tregs failed to exert this effect (Fig. 4G, figs. S10 to S13, and SOM text). Activated FIC Tregs (but

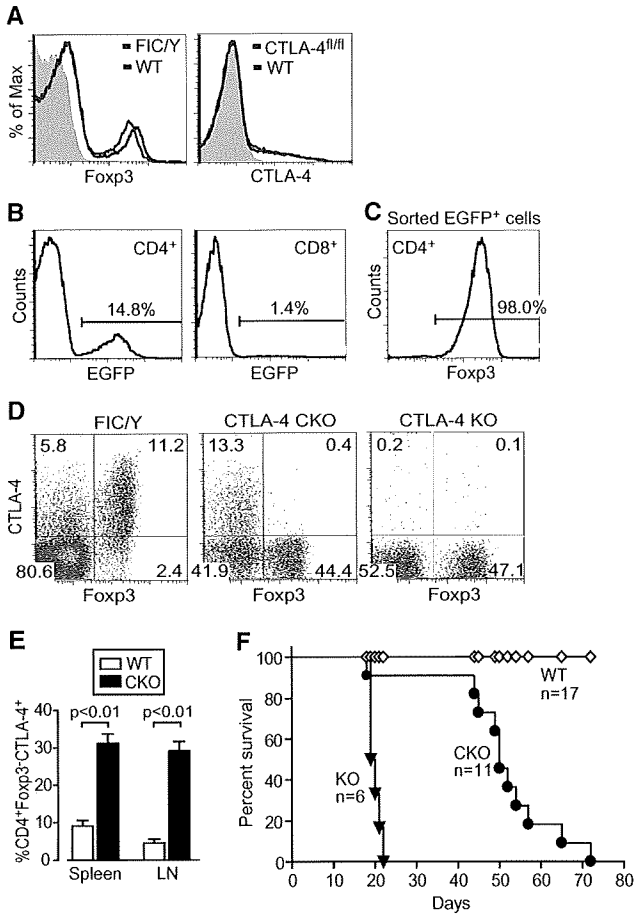

Fig. 1. Specific deletion of CTLA-4 expression in $Foxp3^+$ T cells results in fatal disease. **(A)** Flow cytometric analysis of intracellular Foxp3 (left) and CTLA-4 (right) in freshly isolated LN $CD4^+$ T cells from male FIC, $CTLA\text{-}4^{fl/fl}$, or BALB/c WT mice. **(B)** EGFP expression in $CD4^+$ or $CD8^+$ T cells derived from male FIC-CAG mice. **(C)** Sorted $CD4^+EGFP^+$ cells in FIC-CAG mice were stained for Foxp3. **(D)** CTLA-4 and Foxp3 expression in LN $CD4^+$ T cells from BALB/c WT, CKO, or KO mice. **(E)** Frequency of CTLA-4–expressing $CD4^+Foxp3^-$ T cells in CKO and normal littermates (n = 5). **(F)** Survival of KO and CKO mice as compared with normal littermates. Data represent three or more independent experiments. Vertical bars indicate SEM.

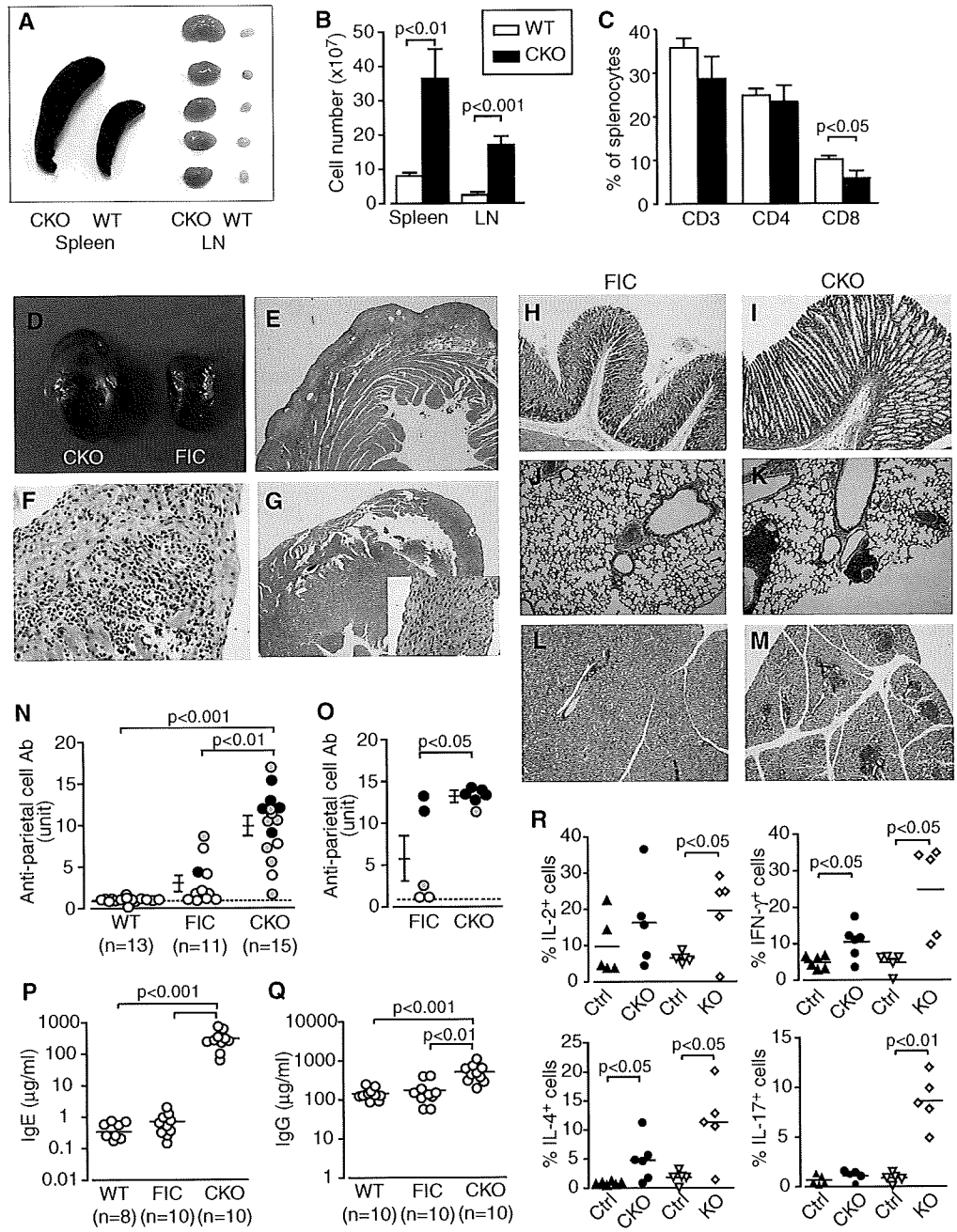

Fig. 2. Autoimmune disease and hyperproduction of IgE in CKO mice. (**A**) Splenomegaly and lymphadenopathy in a CKO and a WT littermate. Lymphocyte numbers (**B**) and frequencies of T cell subsets (**C**) in spleens of 6- to 10-week-old CKO and WT littermates (n = 11 to 13). (**D**) The heart of a CKO (left) and a FIC$^{+/-}$CTLA-4$^{fl/fl}$ mouse (right). Histology (hematoxylin and eosin staining) of the heart of a CKO [(**E** and **F**) ×50 and ×200, respectively] and a FIC mouse [(**G**) ×50; inset, ×200]. Histology of the stomach [(**H** and **I**) ×100], lung [(**J** and **K**) ×100], and salivary gland [(**L** and **M**) ×50] of a CKO [(H), (J), and (L)] and a FIC mouse [(I), (K), and (M)]. Serological and histological development of gastritis in WT, FIC$^{+/+}$, and CKO mice (**N**), and BALB/c nu/nu mice 7 weeks after cell transfer from CKO or FIC$^{+/+}$ mice (**O**). Gastric lesions were histologically graded as 2 (black circle), 1 (gray circle), and 0 (open circle) (*19*). Serum concentrations of IgE (**P**) and IgG (**Q**) in indicated groups of mice. (**R**) Frequencies of cytokine-producing cells among CD4$^+$Foxp3$^-$ splenocytes of 6- to 9-week-old CKO, 16- to 20-day-old KO, or normal littermates (n = 5 to 6). Error bars indicate SEM.

not activated CKO Tregs) also reduced the expression of CD86-GFP fusion protein retrovirally expressed in L-cells, a fibroblast cell line (Fig. 4H). This indicates that Treg-dependant modulation of CD86 expression on DCs is at least partly due to down-regulation of the expression and not masking of the molecule by soluble CTLA-4. Taken together, Treg-mediated CD80/CD86 down-regulation may limit the activation of naive T cells via CD28, resulting in specific immune suppression and tolerance.

Thus, CTLA-4 expressed in Foxp3$^+$ Tregs is critically required for their in vivo and in vitro suppression, which is mediated at least in part by

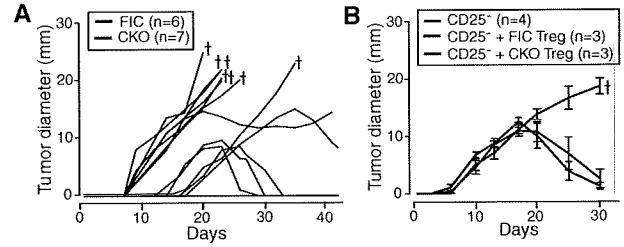

Fig. 3. Treg-specific CTLA-4 deficiency promotes tumor immunity. (**A**) BALB/c nu/nu mice received 3 × 10^7 splenocytes from FIC or CKO mice, followed by intradermal inoculation of 1.5 × 10^5 RLσ1 leukemia cells. Crosses indicate death due to tumor growth. (**B**) BALB/c CD25$^-$ cells (1.5 × 10^7) were cotransferred with 3.8 × 10^5 CD25^{high}CD4$^+$ T cells from CKO or FIC mice and inoculated with 1.5 × 10^5 RLσ1 cells (n = 3). Tumor diameters were measured every other day for 6 weeks. Mice were euthanized when tumor diameters exceeded 20 mm. Error bars indicate SEM.

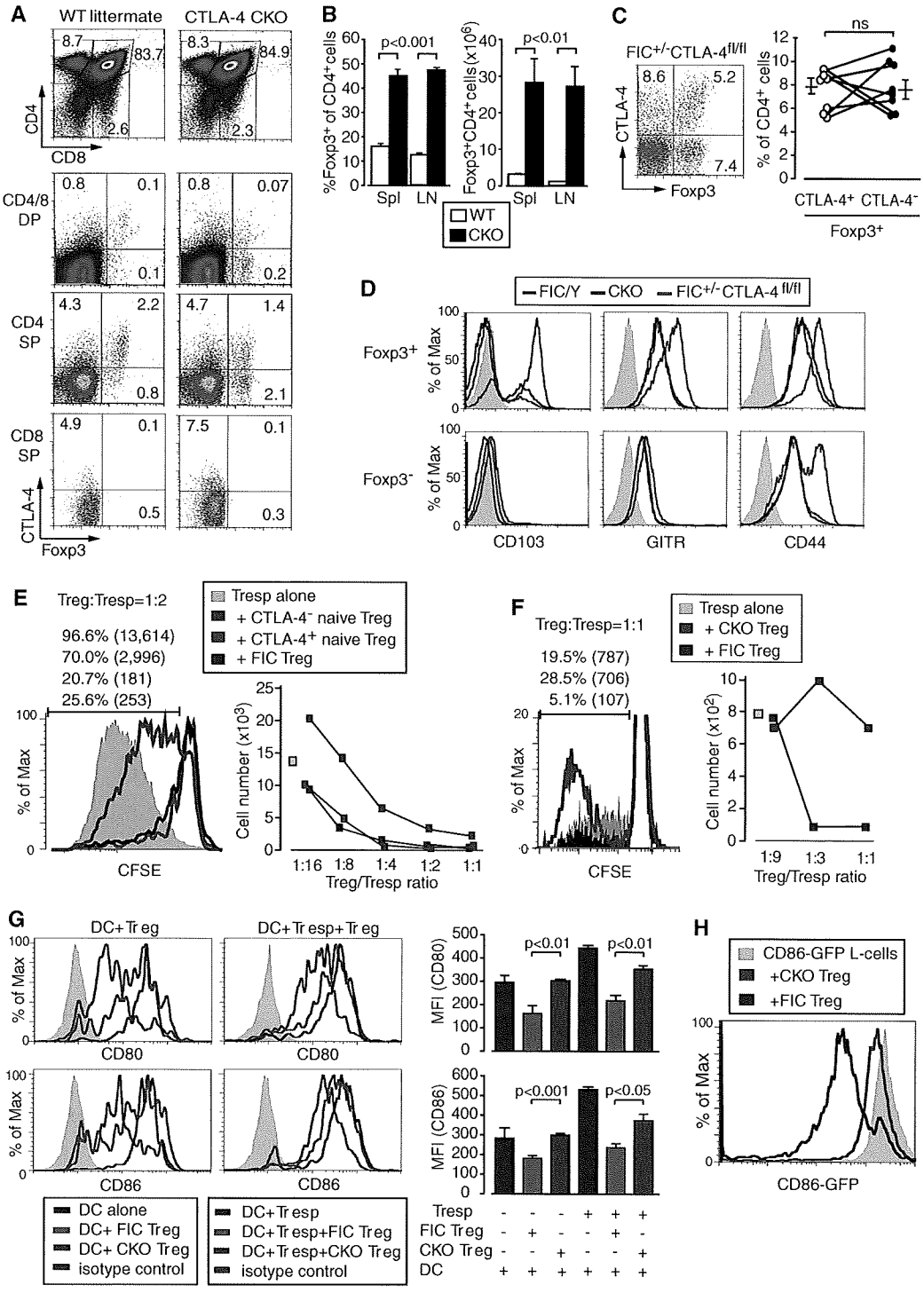

Fig. 4. CTLA-4–deficient Tregs develop and survive normally but have defective function. (**A**) Thymocyte expression of Foxp3 and CTLA-4 in a 2.5-week-old CKO or a WT littermate. SP, single positive; DP, double positive. (**B**) Frequency and number of $CD4^+Foxp3^+$ T cells in spleens and LNs of 6- to 8-week-old CKO or WT littermates (n = 7). (**C**) Foxp3 and CTLA-4 expression in splenic $CD4^+$ T cells from a $FIC^{+/-}CTLA\text{-}4^{fl/fl}$ female mouse (left). Percentages of $Foxp3^+CTLA\text{-}4^+$ and $Foxp3^+CTLA\text{-}4^-$ T cells in each mouse (5 to 8 weeks of age) are connected (n = 8) (right). ns, not significant. (**D**) Expression of cell surface molecules on $CD4^+$ LN cells from CKO, FIC, or $FIC^{+/-}CTLA\text{-}4^{fl/fl}$ mice. (**E**) $CD25^{high}EGFP^+$ cells (naive $CTLA\text{-}4^-$ Treg) and $CD25^{high}EGFP^-$ cells (naive $CTLA\text{-}4^+$ Treg) from $FIC^{+/-}CTLA\text{-}4^{fl/fl}CAG$ female mice and $CD25^{high}CD4^+$ T cells from FIC mice (FIC Treg) were cocultured with $CD25^-CD4^+$ T cells (Tresp), anti-CD3 mAb, and live splenic DCs for 3 days. Percentages and numbers (in parentheses) of CFSE-diluting Tresp cultured at a 1:2 Treg-to-Tresp ratio (left). Numbers of CFSE-diluting Tresp cultured at graded ratios of Treg:Tresp (right). (**F**) Percentage and numbers of CFSE-labeled BALB/c Tresp cocultured with CKO or FIC Tregs and X-irradiated C57BL/6 splenocytes for 4 days at 1:1 Treg:Tresp ratio (left) and numbers at graded ratios (right). (**G**) CD80 and CD86 expression of live splenic DCs after a 2-day culture with Tresp, $CD4^+EGFP^+$ Tregs, or a mix thereof, and anti-CD3 mAb. Histograms show mean fluorescence intensity (MFI). (**H**) L-cells, expressing the Fc receptor, were retrovirally transduced to express CD86-EGFP fusion protein, cocultured with indicated Tregs and anti-CD3 mAb for 2 days, and assessed for GFP level. Data in (A) and (D) to (H) represent three or more independent experiments. Error bars indicate SEM.

CTLA-4–dependent down-regulation of CD80 and CD86 on antigen presenting cells. Tregs probably use multiple suppressive mechanisms, and the importance of each one may vary depending on the environment and the context of immune responses (*1*). However, if the CTLA-4–mediated mechanism of suppression is defective, Tregs cannot sustain self-tolerance and immune homeostasis, even if other suppressive mechanisms become more active to compensate for the deficiency. Thus, CTLA-4 is a key molecular target for controlling Treg-suppressive function in both physiological and pathological immune responses including autoimmunity, allergy, and tumor immunity.

References and Notes

1. S. Sakaguchi *et al.*, *Cell* **133**, 775 (2008).
2. B. Salomon *et al.*, *Immunity* **12**, 431 (2000).
3. T. Takahashi *et al.*, *J. Exp. Med.* **192**, 303 (2000).
4. S. Read, V. Malmstrom, F. Powrie, *J. Exp. Med.* **192**, 295 (2000).
5. S. Hori, T. Nomura, S. Sakaguchi, *Science* **299**, 1057 (2003), published online 9 January 2003; 10.1126/science.1079490.

6. Y. Wu *et al.*, *Cell* **126**, 375 (2006).
7. A. Marson *et al.*, *Nature* **445**, 931 (2007).
8. Y. Zheng *et al.*, *Nature* **445**, 936 (2007).
9. M. Ono *et al.*, *Nature* **446**, 685 (2007).
10. P. Waterhouse *et al.*, *Science* **270**, 985 (1995).
11. E. A. Tivol *et al.*, *Immunity* **3**, 541 (1995).
12. The Wellcome Trust Case Control Consortium, *Nature* **447**, 661 (2007).
13. D. R. Leach, M. F. Krummel, J. P. Allison, *Science* **271**, 1734 (1996).
14. G. Q. Phan *et al.*, *Proc. Natl. Acad. Sci. U.S.A.* **100**, 8372 (2003).
15. S. Read *et al.*, *J. Immunol.* **177**, 4376 (2006).
16. D. M. Sansom, L. S. Walker, *Immunol. Rev.* **212**, 131 (2006).
17. Materials and methods are available as supporting material on *Science* Online.
18. S. Kawamoto *et al.*, *FEBS Lett.* **470**, 263 (2000).
19. M. Ono, J. Shimizu, Y. Miyachi, S. Sakaguchi, *J. Immunol.* **176**, 4748 (2006).
20. Y. Y. Wan, R. A. Flavell, *Nature* **445**, 766 (2007).
21. J. Shimizu, S. Yamazaki, S. Sakaguchi, *J. Immunol.* **163**, 5211 (1999).
22. L. Cederbom, H. Hall, F. Ivars, *Eur. J. Immunol.* **30**, 1538 (2000).
23. C. Oderup, L. Cederbom, A. Makowska, C. M. Cilio, F. Ivars, *Immunology* **118**, 240 (2006).
24. S. Yamazaki, K. Inaba, K. V. Tarbell, R. M. Steinman, *Immunol. Rev.* **212**, 314 (2006).
25. R. J. DiPaolo *et al.*, *J. Immunol.* **179**, 4685 (2007).
26. Y. Onishi *et al.*, *Proc. Natl. Acad. Sci. U.S.A.* **105**, 10113 (2008).
27. We thank M. Ono for discussion and R. Ishii and M. Matsushita for technical assistance. This work was supported by Grants-in-Aid from the Ministry of Education, Sports and Culture of Japan, Japan Science and Technology Agency. Z.F. was a Japan Society for the Promotion of Science fellow, and K.W. was granted a fellowship by Astra-Zeneca, Loughborough, UK.

Supporting Online Material
www.sciencemag.org/cgi/content/full/322/5899/271/DC1
Materials and Methods
SOM Text
Figs. S1 to S13
References

5 May 2008; accepted 15 August 2008
10.1126/science.1160062

Environmental Genomics Reveals a Single-Species Ecosystem Deep Within Earth

Dylan Chivian,[1,2*] Eoin L. Brodie,[2,3] Eric J. Alm,[2,4] David E. Culley,[5] Paramvir S. Dehal,[1,2] Todd Z. DeSantis,[2,3] Thomas M. Gihring,[6] Alla Lapidus,[7] Li-Hung Lin,[8] Stephen R. Lowry,[7] Duane P. Moser,[9] Paul M. Richardson,[7] Gordon Southam,[10] Greg Wanger,[10] Lisa M. Pratt,[11,12] Gary L. Andersen,[2,3] Terry C. Hazen,[2,3,12] Fred J. Brockman,[13] Adam P. Arkin,[1,2,14] Tullis C. Onstott[12,15]

DNA from low-biodiversity fracture water collected at 2.8-kilometer depth in a South African gold mine was sequenced and assembled into a single, complete genome. This bacterium, *Candidatus Desulforudis audaxviator*, composes >99.9% of the microorganisms inhabiting the fluid phase of this particular fracture. Its genome indicates a motile, sporulating, sulfate-reducing, chemoautotrophic thermophile that can fix its own nitrogen and carbon by using machinery shared with archaea. *Candidatus Desulforudis audaxviator* is capable of an independent life-style well suited to long-term isolation from the photosphere deep within Earth's crust and offers an example of a natural ecosystem that appears to have its biological component entirely encoded within a single genome.

A more complete picture of life on, and even in, Earth has recently become possible by extracting and sequencing DNA from an environmental sample, a process called environmental genomics or metagenomics (*1*–*8*). This approach allows us to identify members of microbial communities and to characterize the abilities of the dominant members even when isolation of those organisms has proven intractable. However, with a few exceptions (*5*, *7*), assembling complete or even near-complete genomes for a substantial portion of the member species is usually hampered by the complexity of natural microbial communities.

In addition to elevated temperatures and a lack of O_2, conditions within Earth's crust at depths >1 km are fundamentally different from those of the surface and deep ocean environments. Severe nutrient limitation is believed to result in cell doubling times ranging from 100s to 1000s of years (*9*–*11*), and as a result subsurface microorganisms might be expected to reduce their reproductive burden and exhibit the streamlined genomes of specialists or spend most of their time in a state of semi-senescence, waiting for the return of favorable conditions. Such microorganisms are of particular interest because they permit insight into a mode of life independent of the photosphere.

One bacterium belonging to the *Firmicutes* phylum (Fig. 1A), which we herein name *Candidatus Desulforudis audaxviator*, is prominent in small subunit (SSU or 16*S*) ribosomal RNA (rRNA) gene clone libraries (*11*–*14*) from almost all fracture fluids sampled to date from depths greater than 1.5 km across the Witwatersrand basin (covering 150 km by 300 km near Johannesburg, South Africa). This bacterium was shown in a previous geochemical and 16*S* rRNA gene study (*11*) to dominate the indigenous microorganisms found in a fracture zone at 2.8 km below land surface at level 104 of the Mponeng mine (MP104). Although Lin *et al.* (*11*) discovered that this fracture zone contained the least-diverse natural free-living microbial community reported at that time, exceeding the ~80% dominance by the methanogenic archaeon IUA5/6 of a comparatively shallow subsurface community in Idaho (*15*), we were nonetheless surprised when the current environmental genomics study revealed only one species was actually present within the fracture fluid. Furthermore, we found that the genome of this organism appeared to possess all of the metabolic capabilities necessary for an independent life-style. This gene complement was consistent with the previous geochemical and thermodynamic analyses at the ambient ~60°C temperature and pH of 9.3, which indicated radiolytically generated chemical species as providing the energy and nutrients to the system (*11*), with formate and H_2 as possessing the greatest potential among candidate electron donors, and sulfate (SO_4^{2-}) reduction as the dominant electron-accepting process (*11*).

DNA was extracted from ~5600 liters of filtered fracture water by using a protocol that has been demonstrated to be effective on a broad range of bacterial and archaeal species, including recalcitrant organisms (*16*). A single, complete, 2.35–megabase pair (Mbp) genome was assembled with a combination of shotgun Sanger sequencing and 454 pyrosequencing (*16*). Similar to other studies that obtained near-complete consensus genomes from environmental samples (*5*, *17*), heterogeneity in the population of the dominant species as measured with single-nucleotide polymorphisms (SNP) was quite low, showing only 32 positions with a SNP observed

[1]Physical Biosciences Division, Lawrence Berkeley National Laboratory, Berkeley, CA 94720, USA. [2]Virtual Institute for Microbial Stress and Survival, Berkeley, CA 94720, USA. [3]Earth Sciences Division, Lawrence Berkeley National Laboratory, Berkeley, CA 94720, USA. [4]Departments of Biological and Civil and Environmental Engineering, Massachusetts Institute of Technology, Cambridge, MA 02139, USA. [5]Energy and Efficiency Technology Division, Pacific Northwest National Laboratory, Richland, WA 99352, USA. [6]Department of Oceanography, Florida State University, Tallahassee, FL 32306, USA. [7]Genomic Technology Program, U.S. Department of Energy (DOE) Joint Genomics Institute, Berkeley, CA 94598, USA. [8]Department of Geosciences, National Taiwan University, Taipei 106, Taiwan. [9]Division of Earth and Ecosystem Sciences, Desert Research Institute, Las Vegas, NV 89119, USA. [10]Department of Earth Sciences, University of Western Ontario, London, ON N6A 5B7, Canada [11]Department of Geological Sciences, Indiana University, Bloomington, IN 47405, USA. [12]Indiana Princeton Tennessee Astrobiology Initiative (IPTAI), NASA Astrobiology Institute, Bloomington, IN 47405, USA. [13]Biological Sciences Division, Pacific Northwest National Laboratory, Richland, WA 99352, USA. [14]Department of Bioengineering, University of California, Berkeley, CA 94720, USA. [15]Department of Geosciences, Princeton University, Princeton, NJ 08544, USA.

*To whom correspondence should be addressed. E-mail: DCChivian@lbl.gov

International Immunology, Vol. 20, No. 10, pp. 1331–1342
doi:10.1093/intimm/dxn091

Arthritis and pneumonitis produced by the same T cell clones from mice with spontaneous autoimmune arthritis

Chiaki Wakasa-Morimoto[1], Tomoko Toyosaki-Maeda[1], Takaji Matsutani[2], Ryu Yoshida[1], Shino Nakamura-Kikuoka[1], Miki Maeda-Tanimura[1], Hiroyuki Yoshitomi[3], Keiji Hirota[3], Motomu Hashimoto[3], Hideyuki Masaki[4], Yoshiki Fujii[5], Tsuneaki Sakata[1], Yuji Tsuruta[1], Ryuji Suzuki[6], Noriko Sakaguchi[3] and **Shimon Sakaguchi[3]**

[1]Discovery Research Laboratories, Shionogi & Co., Ltd, 2-5-1 Mishima Settsu-shi, Osaka 566-0022, Japan
[2]Department of Cell Biology, Tohoku University School of Medicine, 2-1 Seiryo-machi, Sendai 980-8575, Japan
[3]Department of Experimental Pathology, Institute for Frontier Medical Sciences, Kyoto University, 53 Shogoin Kawahara-cho, Sakyo-ku, Kyoto 606-8507, Japan
[4]Department of Biochemistry, Kinki University School of Medicine, 377-2 Ohno-higashi, Osakasayama-shi, Osaka 589-8511, Japan
[5]Department of Virology 1, National Institute of Infectious Diseases, 1-23-1 Toyama, Shinjuku-ku, Tokyo 162-8640, Japan
[6]Clinical Research Center for Rheumatology and Allergy National Sagamihara Hospital, 18-1 Sakuradai, Sagamihara-shi, Kanagawa 228-8522, Japan

FEATURED ARTICLE

Keywords: animal model, interstitial lung disease, rheumatoid arthritis, T cell clone

Abstract

SKG mice, a newly established model of rheumatoid arthritis (RA), spontaneously develop autoimmune arthritis accompanying extra-articular manifestations, such as interstitial pneumonitis. To examine possible roles of T cells for mediating this systemic autoimmunity, we generated T cell clones from arthritic joints of SKG mice. Two distinct $CD8^+$ clones were established and both showed *in vitro* autoreactivity by killing syngeneic synovial cells and a variety of MHC-matched cell lines. Transfer of each clone to histocompatible athymic nude mice elicited joint swelling and histologically evident synovitis accompanying the destruction of adjacent cartilage and bone. Notably, the transfer also produced diffuse severe interstitial pneumonitis. Clone-specific TCR gene messages in the inflamed joints and lungs of the recipients gradually diminished, becoming hardly detectable in 6–11 months; yet, arthritis and pneumonitis continued to progress. Thus, the same $CD8^+$ T cell clones from arthritic lesions of SKG mice can elicit both synovitis and pneumonitis, which chronically progress and apparently become less T cell dependent in a later phase. The results provide clues to our understanding of how self-reactive T cells cause both articular and extra-articular lesions in RA as a systemic autoimmune disease.

Introduction

Rheumatoid arthritis (RA) is a chronic inflammatory disease of unknown etiology that primarily affects the synovial membranes of multiple joints (1, 2). A cardinal feature of joint inflammation in RA is proliferative inflammation of the synovium, i.e. synovitis, which leads to the destruction of adjacent cartilage and bone. In addition, RA frequently accompanies extra-articular manifestations, for example the development of rheumatoid factors, rheumatic nodules, vasculitis and interstitial lung disease (ILD). Recent studies with high-resolution imaging have indeed revealed a high prevalence of ILD in patients with RA (3–6). RA is thus a systemic disease; yet, the immunological basis of this systemic autoimmunity is poorly understood.

T cells appear to play a key role in the development of RA as suggested by the infiltration of T cells, especially $CD4^+$ T cells, into the synovial tissue of RA (7–9) and the association of genetic susceptibility to RA with particular alleles of HLA-DR (10, 11). On the other hand, there is evidence in humans and animal models that stimulated synoviocytes, composed of macrophage-like and fibroblast-like synovial cells, can

Correspondence to: S. Sakaguchi; E-mail: shimon@frontier.kyoto-u.ac.jp

Transmitting editor: K. Yamamoto

Received 31 March 2008, *accepted* 17 July 2008

Advance Access publication 18 August 2008

themselves mediate joint destruction in a T cell-independent manner (12, 13). A key issue in elucidating the pathogenetic mechanism of RA is, therefore, to determine how self-reactive T cells contribute to the initiation and progression of synovitis and possibly extra-articular lesions such as ILD.

The SKG strain of mice spontaneously develops T cell-mediated chronic autoimmune arthritis (14–16). The strain possesses a mutation in the gene encoding a Src homology 2 domain of the ζ-associated protein of 70 kDa (ZAP-70), a key signal transduction molecule in T cells (17, 18). Impaired signal transduction through SKG ZAP-70 results in thymic positive selection and failure in negative selection of highly self-reactive T cells that include potentially arthritogenic T cells (14). The SKG arthritis progresses chronically, starting from small joints of the digits and symmetrically progressing to larger joints, such as the wrists and ankles. Histologically, affected joints show hyperplasia of synoviocytes, inflammatory cell infiltration, pannus formation and destruction of cartilage and bone, eventually leading to joint deformity. As extra-articular lesions, they develop interstitial pneumonitis, dermatitis, necrobiotic nodules akin to rheumatic nodules in RA and systemic vasculitides. Serologically, they spontaneously develop IgM-type rheumatoid factors, auto-antibodies against type II collagen and antibodies cross-reactive with *Mycobacterium tuberculosis* heat shock protein (hsp) 70. IL-1, tumor necrosis factor (TNF)-α, IL-6 or IL-17 deficiency inhibits the development of arthritis in SKG mice (15, 19), similar to the effects of anti-cytokine therapies in RA (20, 21). Thus, autoimmune disease in SKG mice closely resembles RA in clinical and immunopathological characteristics. In addition, considering recent findings that genetic polymorphism of a signaling molecule at a TCR proximal step involving ZAP-70 significantly contributes to the susceptibility to RA and other autoimmune diseases (22, 23), SKG mice can be a suitable model for elucidating how a T cell-intrinsic anomaly contributes to the development of RA as a systemic autoimmune disease.

In this study, we have attempted to determine the role of T cells in SKG autoimmune disease by establishing T cell clones from their arthritic lesions. We have established two distinct $CD8^+$ clones and show that both of them have the potential to induce not only arthritis but also pneumonitis. This indicates that inflammation in both the joints and the lung can be mediated, at least in part, by common autoreactive T cell clones in SKG mice. In addition, by adoptively transferring these T cell clones to normal mice, we show that autoreactive T cells are able to initiate arthritis; yet, the arthritis can progress apparently in a T cell-independent manner in a later phase. These findings contribute to our understanding of how T cells cause chronic arthritis and ILD in RA.

Materials and methods

Mice

SKG and (SKG × BALB/c)F_1 mice (14) were maintained in the animal facility of Kyoto University under a microbially conventional condition. Female C.B-17 SCID mice (Clea Japan, Tokyo, Japan), DBA/1J, BALB/c and BALB/c-nu/nu mice (Charles River Japan, Kanagawa, Japan) were maintained under specific pathogen-free conditions at Kyoto University or Discovery Research Laboratories of Shionogi & Co., Ltd. All experiments were approved by the Animal Care and Use Committee at Kyoto University and Shionogi & Co., Ltd.

Culture medium

The culture medium for SKG T cell lines and clones was AIM-V supplemented with 20% RPMI-1640, 1 mM sodium pyruvate, 50 μM 2-mercaptoethanol (ME), 2 mM L-glutamine, ×1 penicillin/streptomysin (Gibco BRL, Gaithersburg, MD, USA), 10% heat-inactivated FCS (Hyclone, Logan, UT, USA), 10% rat T-STIM™ with Con A (Becton Dickinson, Franklin Lakes, NJ, USA), 100 U/ml of recombinant mouse IL-2 (Genzyme, Cambridge, MA) and 5 μg/ml of Con A (Sigma, St Louis, MO, USA).

Establishment of T cell clones from arthritic joints of SKG mice

To establish T cell lines, severely swollen joints of SKG mice were aseptically excised, finely minced and cultured until clusters of mononuclear cells were confirmed in bulk culture. Outgrown T cells were cloned in 96-well microplates by using SKG synovial cells (1×10^3) as feeder cells. Synovial cells were prepared as previously described (16). Briefly, synovial tissues from wrist and ankle joints were digested with 400 Mandl U/ml of Liberase Brendzyme II (Roche) in RPMI-1640 medium for 1 h at 37°C; digested cells were filtrated through a nylon mesh to prepare single-cell suspensions. A typical composition of the synoviocyte preparation was ~10% $CD11b^+$ monocyte/macrophages, ~20% $Gr\text{-}1^+$ granulocytes, ~1% T cells and other cells. Several days later non-adherent cells were removed by washing the plates with culture medium. T cells that had outgrown from the bulk culture of synovial cells were dispensed at 1, 5, 20 or 50 cells per well and apparently single colonies were propagated in the culture medium described above. Clonality of each cell was confirmed by microplate hybridization assay (MHA) (24) and sequence analysis of TCR. Established T cell clones were maintained without feeder cells. Dengue 2F7 and 3F2 T cell clones, established by immunization of BALB/c mice with the NS3 peptide of dengue virus, were kindly provided by Dr H. Masaki (Kinki University). All cultures were performed in a humidified atmosphere of 7.5% CO_2 at 37°C.

Cytokine detection

Cytokine production by T cell clones were analyzed by ELISA. T cell clones were stimulated with 10 ng/ml of phorbol myristate acetate (PMA) (Wako Chemicals USA, Inc., Richmond, VA, USA) and 0.4 μg/ml of ionomycin (Calbiochem, Darmstadt, Germany) in culture medium at 1×10^6 cells/ml for 16 h. The supernatants were assayed for various cytokines using specific ELISA kits (Endogen, Woburn, MA, USA, and Axis-Shield, Oslo, Norway) according to the manufacturer's protocol. Cytokine mRNA levels in the joints and lungs of clone recipient mice were analyzed by quantitative PCR as described previously (25).

MHA for TCR AV and BV family and sequence analysis

MHA, cDNA synthesis and PCR amplifications of TCR of each T cell clone were performed as described previously (24). The

PCR products cloned into a pGEM-T Easy vector (Promega, Madison, WI, USA) were analyzed for TCR sequences using CEQ DTCS-Quick Start Kit according to the manufacturer's protocol (Beckman Coulter Inc., Fullerton, CA, USA).

^{51}Cr release cytotoxicity assay

BALB/3T3 fibroblast line (H-2^d), J774 macrophage line (H-2^d), p815 mastocytoma line (H-2^d), EL-4 lymphoma line (H-2^b), L929 fibroblast line (H-2^k) obtained from Dainippon Sumitomo Pharma (Osaka, Japan) and synovial cells of SKG mice (H-2^d) were used as target cells. Synovial cells (1×10^4) were seeded in 96-well flat-bottom plates with 40 U/well of IFN-γ for 2 days and radiolabeled with 2.5 μCi/well of $Na_2^{51}CrO_4$ (Daiichi Radioisotope Laboratories, Ltd, Tokyo, Japan) for 2 h. Other target cells (3×10^5) were radiolabeled with 20 μCi of $Na_2^{51}CrO_4$ for 2 h and seeded in 96-well round-bottom plates at 1×10^4 cells per well. Effector cells (4×10^5) were added in each well in triplicate and incubated for 8 h. Relative cytotoxicity was calculated as follows from the radioactivity released in the culture supernatant; percent specific lysis = 100(experimental − spontaneous)/(maximal − spontaneous) counts per minute. Maximal lysis and spontaneous release were determined from target cells incubated with surfactant ×7 (Flow Laboratories, ICN Biomedicals, Inc., Aurora, OH, USA) or without effector cells, respectively.

Adoptive transfer

Spleen T cells from SKG mice or (SKG × BALB/c)F_1 mice and each SKG T cell clones (1×10^7) were intravenously transferred to C.B-17 SCID mice (8 weeks) or BALB/c-nu/nu mice (6 weeks), respectively. Control dengue 2F7 and 3F2 clone were collected 10–14 days after *in vitro* stimulation with specific peptide-pulsed irradiated (33 Gray) BALB/c spleen cells and transferred as described above. Severity of arthritis was scored weekly as previously described (14).

Clinical assessment of arthritis

Joint swelling was monitored by inspection and scored as follows: 0, no joint swelling; 0.1, swelling of one finger joint; 0.5, mild swelling of wrist or ankle and 1.0, severe swelling of wrist or ankle. Scores for all fingers and toes, wrists and ankles were totalled for each mouse (14).

Histological assessment of interstitial pneumonitis

Interstitial pneumonitis was evaluated microscopically depending on diffusely affected area: –, normal histology; +, 10–30%; ++, 30–60%; +++, >60% of the sections of the lungs showed pneumonitis.

Histology and immunohistochemistry

Tissues were fixed in 10% neutral formalin, paraffin embedded and stained with Haematoxylin & Eosin (H&E). Joints were additionally decalcified for 3 weeks in 10% EDTA in PBS before staining. For immunohistochemistry of joints, deparaffinized sections were incubated with 20% normal rabbit serum (Dako, Hamburg, Germany) in PBS for 15 min to block non-specific binding, primary rat anti-Ly-6G mAb (Gr-1, RB6-8C5; BD PharMingen) with appropriate dilutions overnight at 4°C, biotinylated polyclonal rabbit anti-rat antibody (Dako) and HRP-conjugated streptavidin (Dako). The slides were developed using diaminobenzidene (Elite Kit; Vector, Burlingame, CA, USA) and counterstained with Mayer's hematoxylin.

For immunohistochemistry of lungs, tissues were fixed in 4% phosphate-buffered PFA (pH 7.4) and embedded in Tissue-Tek OCT compound (Ted Pella, Inc., Redding, CA, USA). Cryostat sections were stained with rat mAbs to mouse CD4 (H129.19), CD8a (53-6.7), CD45R/B220 (RA3-6B2), Ly-6G (RB6-8C5) (BD PharMingen) and F4/80 (Cl: A3-1) (CALTAG Laboratories, Burlingame, CA, USA) with appropriate dilutions followed by incubation with biotinylated secondary antibodies and HRP-conjugated streptavidin. The slides were developed as described above.

Southern blot analysis

The persistence of transferred clones in the recipients was assessed by Southern blot analysis. Two micrograms of total RNA of each tissue was treated with DNaseI and reverse transcribed using Superscript II (Invitrogen, Carlsbad, CA, USA). Nested PCRs were performed as described previously (24) to amplify TCR β chain of 35S or dengue 2F7 with the primers specific for V, J and C region. Ten microliters of the PCR products were separated on 2% agarose gel, transferred onto Hybond-N+ membranes (Amersham Biosciences, Piscataway, NJ, USA) according to the manufacturer's instructions. The membranes were prehybridized overnight with PerfectHyb (TOYOBO CO., Ltd, Osaka, Japan) at 54°C and hybridized with the third complementarity-determining region (CDR3)-specific probes labeled with ^{32}P-deoxyadenosine triphosphate for 3 h at 54°C. The membranes were washed in ×2 standard saline citrate (SSC) and 0.1% SDS at room temperature and ×0.2 SSC and 0.1% SDS at 37°C. RNA extracts of 35S and dengue 2F7 clones, diluted to 1% of concentration with RNA of L9 cells, were used as positive controls. The detection limits of 35S and dengue 2F7 were compared using the serial dilution of positive controls and both systems detected the RNA extract corresponding to the amount of one cell.

The sequences of PCR primers and probes are as follows; 35S: first PCR (BV8S3-1: 5′-ATA TGG TGC TGG CAA CCT TC-3′ and MCB1: 5′-AGG ATT GTG CCA GAA GGT AG-3′), second PCR (BV8S3-2: 5′-ACC AGA ACA ACG CAA GAA GAC T-3′ and MCB2: 5′-TTG TAG GCC TGA GGG TCC-3′), third PCR (BV8S3-3: 5′-TTC CTC CTG CTG GAA TTG GC-3′ and BJ1.5: 5′-TAG AAC AGA GAT CGA GTC CC-3′) and probe (5′-AGT GGG ACA GGG GGC AAC CA-3′). Dengue 2F7: first PCR (BV8S1-1: 5′-CCC AAA GTC CAA GAA GCA AG-3′ and MCB1), second PCR (BV8S1-2: 5′-GTA CAA GGC CTC CAG ACC AA-3′ and MCB2), third PCR (BV8S1-3: 5′-TGG CTT CCC TTT CTC AGA CA-3′ and BJ2.7: 5′-AAG GAG ACC TTG GGT GGA GT-3′) and probe (5′-TGC CAC CAA CGA CAA CTC CT-3′).

Results

Induction of arthritis and interstitial pneumonitis in SCID mice by the transfer of SKG splenic T cells

In our conventional housing environment, SKG mice started to develop arthritis around 2 months of age and

histologically evident mild interstitial pneumonitis around 6 months of age (14). To determine the role of T cells in SKG mouse autoimmunity, we transferred splenic T cells from 3-month-old arthritic SKG mice (without histologically evident pneumonitis or colitis) to T/B-cell-deficient C.B-17 SCID mice, which are histocompatible with SKG mice on the BALB/c background (14). Within 2 months after transfer, the recipient developed arthritis (14) and mild but histologically evident interstitial pneumonitis (Table 1, Fig. 1); they also developed mild colitis (data not shown). Similar cell transfer from non-arthritic heterozygotes of the SKG mutation failed to induce such lesions in the recipients. Age-matched SCID mice similarly maintained in our facility did not develop these lesions histologically (data not shown). The results thus indicate that SKG T cells are able to adoptively transfer arthritis and also have a potential to induce interstitial pneumonitis and colitis when transferred to SCID mice.

Establishment of T cell clones from arthritic joints

To analyze the mechanism of such T cell-mediated inflammatory tissue damage in multiple organs, we attempted to establish T cell clones from arthritic joints of SKG mice, as described in Materials and methods. Two T cell clones, designated 35S and 73S, were established in separate experiments. The clones were maintained and expanded with culture medium containing IL-2 and Con A (see Materials and methods). $CD8^+$ CTL clones specific for dengue virus NS3 protein were used as control.

Cytofluorometric analyses revealed that the 35S and 73S clones were $CD8^+$. Both expressed α and β chains of the TCR, and the expression level of the TCR on 35S was slightly lower than normal (Fig. 2). In response to *in vitro* PMA and ionomycin stimulation, 35S and 73S produced IFN-γ but no detectable amount of TNF-α, IL-4, IL-5, IL-6, IL-10 or IL-17 by ELISA (Table 2).

Clonality of each T cell line was confirmed by MHA (24) (data not shown) and sequence analysis of the TCR α and β chains with determination of the amino acid sequences of the TCRs (Table 3). Interestingly, these T cell clones shared in common the BV8S3 TCR Vβ subfamily; yet, the CDR3 sequences of the TCR β chains were different (26–29).

Table 1. Induction of arthritis, interstitial pneumonitis and colitis in SCID mice by the transfer of SKG splenic T cells

Spleen cell donor	Recipients	Arthritis	Interstitial pneumonitis	Colitis
SKG	1	++ (4.6)	++	+
	2	++ (4.0)	++	+
	3	++ (4.0)	+	+
	4	++ (3.0)	+	−
(SKG × BALB/c)F_1	1	−	−	−
	2	−	−	−
	3	−	−	−
	4	−	−	−

Cells (1×10^7) of T cells prepared from spleens of indicated mice were intravenously transferred to 8-week-old SCID mice. The severity of arthritis, interstital pneumonitis and colitis in these mice was histologically assessed 2 months later.

Autoreactivity of T cell clones

In ^{51}Cr release cytotoxicity assay to determine cytotoxic activity of the SKG clones against syngeneic synovial cells, 35S and 73S lysed SKG synovial cells prepared by crude collagenase digestion of inflamed synovium (44.0 and 16.3% of specific lysis, respectively, at a high 40:1 ratio), while control dengue 2F7 clone did not (Fig. 3A). 35S lysed not only syngeneic synovial cells but also MHC-matched cell lines, such as BALB/c-derived 3T3 cells, macrophage-like J774 cells and DBA/2 (H-2^d)-derived P815 cells, whereas the clone failed to lyse allogenic EL-4 (H-2^b) lymphoid or L929 (H-2^k) fibroblast cell line (Fig. 3B). Thus, 35S appears to recognize a ubiquitous self-peptide in an MHC-restricted manner. These

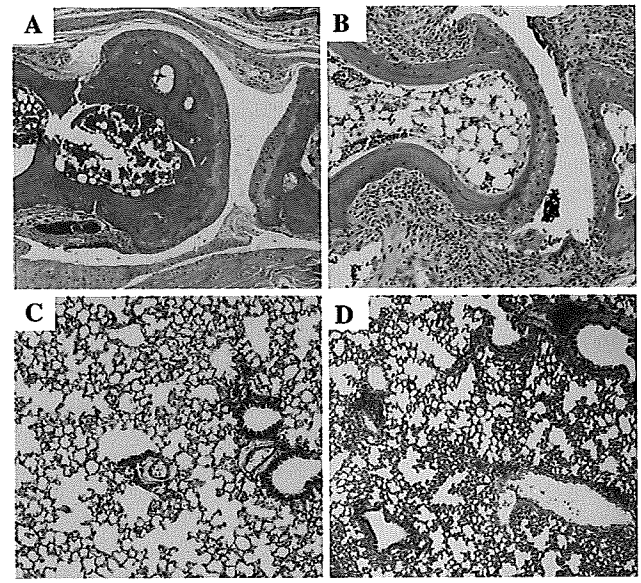

Fig. 1. Arthritis and pneumonitis in SCID mice transferred with T cells from SKG mice. Histology of a joint (A) and lung (C) of a SCID mouse T cell transferred from (SKG × BALB/c)F_1 mouse. Arthritis (B) and interstitial pneumonitis (D) in a SCID mouse T cell transferred from a SKG mouse. H&E staining (A and B, ×100; C and D, ×50).

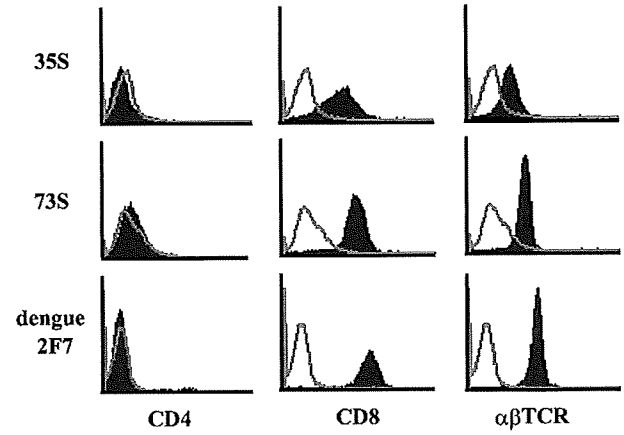

Fig. 2. Expression levels of CD4, CD8 and αβ TCR on 35S, 73S and dengue 2F7 clones.

functional characteristics, together with cell surface and cytokine-secreting profiles, indicate that 35S and 73S are CTL and that they bear self-reactive specificity.

Induction of synovitis in BALB/c nude mice by adoptive transfer of T cell clones

To examine possible arthritogenicity of the T cell clones, they were transferred to BALB/c nude mice once, and the degree of joint swelling of each recipient mouse was assessed once a week for 12 months (Fig. 4). Transfer of 35S and 73S clones induced joint swelling with incidences of 57.1% (4 out of 7 mice) and 42.9% (3 out of 7 mice), respectively, during the observation period; synovitis was histologically evident in 71.4% (5 out of 7 mice) in each transfer (Table 4, Fig. 5). Once joint swelling started in one joint following cell transfer, it slowly progressed with remissions and exacerbations, leading to swelling of other joints in a symmetrical fashion (Figs 4 and 5A–D). Two mice showed progressive debilitation to death without an apparent cause, although one of them showed dermatitis; with debilitation, joint swelling somehow remitted in these mice.

Histologically, swollen joints showed marked synovial and peri-articular inflammation when examined 6–12 months after cell transfer (Fig. 5E and F). The inflammation accompanied a marked proliferation of synovial lining cells, infiltration of inflammatory cells into subsynovial tissue and joint cavity and active angiogenesis; pannus eroded the adjacent cartilage and bone (Fig. 5F). Gr-1-positive neutrophils were abundant among the infiltrating cells, as observed in the arthritic lesions of SKG mice (14, 15), whereas few T cells infiltrated into the inflammation sites (Fig. 5G and H).

In accordance with the appearance of multinuclear cells at the interface between proliferating synoviocytes and bone, many tartrate-resistant acid phosphatase-positive osteoclasts were observed in the inflamed joints (Fig. 6A–D). Safranin-O staining revealed a decrease in proteoglycan in the articular cartilage matrix of severely affected joints (Fig. 6E and F). Notably, Gr-1-positive cells, mainly neutrophils, also increased in the bone marrow (BM) of the affected recipients (Fig. 6G and H).

A high level of circulating rheumatoid factors was detected in one mouse out of seven recipients of the 35S clone and in none of the recipients of other clones (data not shown).

Some of the swollen joints following transfer of 35S $CD8^+$ clones exhibited higher expression levels of IL-17 mRNA assessed by quantitative reverse transcription (RT)–PCR than those from mice transferred with control $CD8^+$ clones (Supplementary Figure 1A, available at *International Immunology* Online), despite that 35S failed to produce IL-17 upon *in vitro* stimulation.

Taken together, the $CD8^+$ T cell clones prepared from arthritic lesions of SKG mice were able to induce arthritis in athymic nude recipients, leading to the destruction of the surrounding cartilage and the bone.

Table 2. Cytokine production (ng/ml) of T cell clones derived from SKG joints and control clones

	TNF-α	IFN-γ	IL-4	IL-5	IL-10	IL-6	IL-17
35S	0.02	180	0.03	<0.02	<0.04	0.2	<0.01
73S	0.02	80	0.03	<0.02	1.2	<0.05	<0.01
Dengue 2F7	0.2	10	ND	ND	<0.04	<0.05	<0.01
Dengue 3F2	0.02	20	ND	ND	<0.04	<0.05	<0.01

Culture supernatant of activated cells by PMA and ionomycin for 16 h were assayed by ELISA. ND, not done.

Table 3. CDR3 sequences of the TCR α and β chain used by the SKG T cell clones

TCR α chains	AV	V	N	J	AJ
35S	3S6	C A V T	S D	S G T Y Q R F	13
73S	3S1	C A A S M	R R	N S G T Y Q R F	13
Dengue 2F7	2S2/7	C A A		N Q G G R A L I F	15
Dengue 3F2	2S2/7	C A A	S G R D	Y A N K M I F	47
TCR β chains	**BV**	**V**	**N-D-N**	**J**	**BJ**
35S	8S3	C A S S G	T G G	N Q A P L F	1.5
73S	8S3	C A S S G	W G D	A E Q F F	2.1
Dengue 2F7	8S1	C A T	N D N	S Y E Q Y E	2.7
Dengue 3F2	8S2	C A S E	T R	E Q Y F	2.6

The amino acid sequences of the V, D and J regions of the TCR were determined according to the nucleotide sequences. AV and BV gene families were assigned according to Arden *et al.* (26). AJ genes were numbered according to Koop *et al.* (27). BJ genes were assigned according to Malissen *et al.* (28) and Gascoigne *et al.* (29).

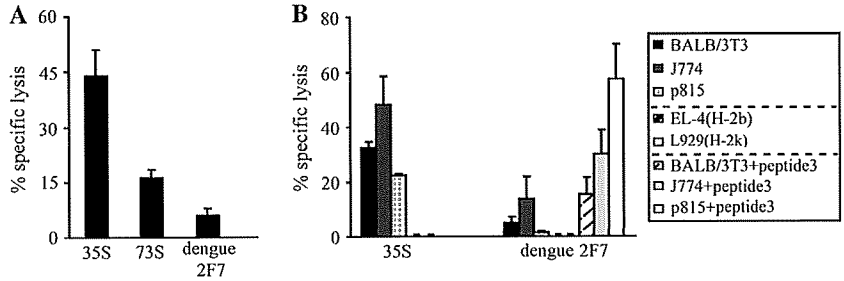

Fig. 3. *In vitro* self-reactivity of SKG T cell clones. (A) CTL activity of SKG T cell clones against SKG synovial cells. CTL clones specific for dengue virus NS3 protein, dengue 2F7, was used as control. IFN-γ-treated target cells were ^{51}Cr labeled in adherent condition and incubated with effector cells for 8 h (E:T ratio = 40). (B) CTL activity of SKG T cell clones against various types of cell lines (E:T ratio = 40). CTL activity of dengue 2F7 clone was also analyzed against $H\text{-}2^d$ cells pulsed with a specific peptide (E:T ratio = 10). All assays were conducted in triplicate with 8 h of incubation. The mean and standard deviation of three independent experiments are shown in each bar.

Induction of interstitial pneumonitis in BALB/c nude mice by the transfer of T cell clones

Notably, histologically evident severe alveolitis and diffuse interstitial pneumonitis also developed in all the recipients of 35S and 73S but not in those recipients of dengue 2F7 and 3F2 clones (Table 4 and Fig. 7A–D). Some recipients of 35S and 73S developed only pneumonitis without histologically evident synovitis. No histologically apparent inflammation was observed in other tissues/organs including the liver and the colon in any of these recipient mice (data not shown). The diffuse pulmonary lesions (Fig. 7A and B) comprised thickening of the alveolar walls, and perivascular and peribronchiolar infiltration by inflammatory cells (Fig. 7C and D). Immunohistochemical analysis of the 73S recipients 6 months after cell transfer revealed the infiltration of a large number of granulocytes as Gr-1$^+$ cells (Fig. 7E), macrophages as F4/80$^+$ cells (Fig. 7F) and B cells as B220$^+$ cells (Fig. 7G) into the alveolar walls and spaces and also the perivascular and peribronchiolar area where only a small number of CD8$^+$ T cells were detected, which might be transferred to CD8$^+$ clones or derived from nude mice (30) (Fig. 7H). CD4$^+$ T cells were occasionally found in the lesions and could be those derived from endogenous T cells that might develop extrathymically in aged nude mice (Fig. 7I) (30).

The pulmonary tissues with severe interstitial pneumonitis following CD8$^+$ clone transfer exhibited higher expression levels of IL-17 mRNA by quantitative RT–PCR compared with the mice transferred with control CD8$^+$ clones (Supplementary Figure 1B, available at *International Immunology* Online).

Thus, the SKG arthritogenic T cell clones are able to induce interstitial pneumonitis when transferred to athymic nude mice.

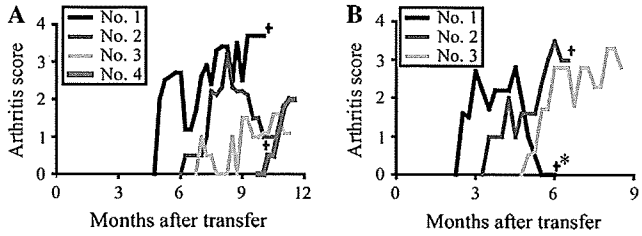

Fig. 4. Time course of joint swelling in the recipient mice of SKG T cell clones, 35S (A) and 73S (B). Score for all paws were totalized for each mouse. +, Sacrificed at the indicated time points; *, the mouse developed dermatitis at 5 months after transfer.

Detection of transferred clones in recipient mice

Since T cells were hardly detected by immunohistochemistry at the site of synovitis or pneumonitis 6 months after clone transfer (data not shown and see above), the persistence of transferred clones in the recipients was assessed by RT–PCR amplification of TCR β chain gene and Southern blot analysis of the products with a CDR3 sequence-specific probe. We adopted this method to avoid detecting nude mouse-derived oligoclonal endogenous T cells that may expand with aging (see above) (30–32). For example, a clone-specific TCR message of the 35S clone was detected in the majority of recipient spleens 1 month after transfer but not in the spleens examined 6 months later (Fig. 8). As shown in Fig. 9, the messages were

Table 4. Development of arthritis and interstitial pneumonitis in BALB/c nude mice transferred with T cell clones

Clone	Individual recipients	Macroscopically evident arthritis			Histological analysis	
		Onset (months)	Sacrifice (months)	Clinical score[a]	Synovitis[b]	Interstitial pneumonitis[c]
35S	1	5	10	3.7	++	+
	2	6	11	3.2	++	++
	3	7	11	1.6	++	+++
	4	10	12	2.0	++	+++
	5	–	9	0	+	±
	6	–	12	0	—	+++
	7	–	12	0	—	+++
73S	1	2.5	6	2.8	++	++
	2	3.5	6	3.5	++	+
	3	5	9	3.3	++	++
	4	–	8	0	+	++
	5	–	9	0	+	+++
	6	–	12	0	—	++
	7	–	12	0	—	++
Dengue 2F7	1	–	9	0	—	—
	2	–	9	0	—	—
	3	–	9	0	—	—
	4	–	9	0	—	—
	5	–	12	0	—	—
	6	–	12	0	—	—
	7	–	12	0	—	—
Dengue 3F2	1	–	12	0	—	—
	2	–	12	0	—	—

Six-week-old BALB/c nude mice were intravenously injected with 1 × 10^7 cells of each clone. The incidence of joint swelling of the recipient mice was examined weekly. Mice were sacrificed 6–12 months after cell transfer.

[a]Maximum clinical score of arthritis.

[b]–, Without change; +, microscopically observed synovitis without joint swelling; ++, macroscopically obvious joint swelling.

[c]–, Normal histology; +, 10–30%; ++, 30–60%; +++, >60% of the sections of the lungs showed pneumonitis (Fig. 7).